Ricean K-Factors in Narrow-Band Fixed Wireless Channels: Theory, Experiments, and Statistical Models

Larry J. Greenstein, *Life Fellow, IEEE*, Saeed S. Ghassemzadeh, *Senior Member, IEEE*, Vinko Erceg, *Fellow, IEEE*, and David G. Michelson, *Senior Member, IEEE*

***Abstract*—Fixed wireless channels in suburban macrocells are subject to fading due to scattering by moving objects such as windblown trees and foliage in the environment. When, as is often the case, the fading follows a Ricean distribution, the first-order statistics of fading are completely described by the corresponding average path gain and Ricean K-factor. Because such fading has important implications for the design of both narrow-band and wideband multipoint communication systems that are deployed in such environments, it must be well characterized. We conducted a set of 1.9-GHz experiments in suburban macrocell environments to generate a collective database from which we could construct a simple model for the probability distribution of K as experienced by fixed wireless users. Specifically, we find K to be lognormal, with the median being a simple function of season, antenna height, antenna beamwidth, and distance and with a standard deviation of 8 dB. We also present plausible physical arguments to explain these observations, elaborate on the variability of K with time, frequency, and location, and show the strong influence of wind conditions on K.**

***Index Terms*—Fading, fixed wireless channels, K-factors, multipoint communication, Ricean distribution.**

I. Introduction

During the past decade, both common carriers and utilities have begun to deploy fixed wireless multipoint communication systems in suburban environments. For common carriers, wideband multipoint communication systems provide a method for delivering broadband voice and data to residences with greater flexibility than wired services. For utilities, narrow-band multipoint communication systems provide a convenient and independent method for controlling or monitoring the infrastructure, including utility meters located on customer premises. In the past, most narrow-band fixed wireless links were deployed in frequency bands below 900 MHz. In response to increasing demand, both the Federal Communication Commission and Industry Canada have recently allocated several new bands between 1.4 and 2.3 GHz to such applications. Because fading on fixed wireless links has important implications for the design of both narrow-band and wideband multipoint communication systems, it must be well characterized. Narrow-band fading models apply to both narrow-band signals and individual carriers or pilot tones in orthogonal frequency-division multiplexing systems such as those based upon the IEEE 802.16 standard. Ideally, such models will capture not just the statistics of fading but their dependence upon the type and density of scatterers in the environment as well.

The complex path gain of any radio channel can quite generally be represented as having a fixed component plus a fluctuating (or scatter) component. The former might be due to a line-of-sight path between the transmitter and the receiver; the latter is usually due to echoes from multiple local scatterers, which causes variations in space and frequency of the summed multipath rays. The spatial variation is translated into a time variation when either end of the link is in motion. In the case of fixed wireless channels, time variation is a result of scatterers in motion.

If the scatter component has a complex Gaussian distribution, as it does in the central limit (many echoes of comparable strength), the time-varying magnitude of the complex gain will have a Ricean distribution. The key parameter of this distribution is the *Ricean K-Factor* (or just K), which is the power ratio of the fixed and scatter components [1]–[3]. It is a measure of the severity of fading. The case $K = 0$ (no fixed component) corresponds to the most severe fading, and in this limiting case, the gain magnitude is said to be Rayleigh distributed. From the earliest days, most analyses of mobile cellular systems, e.g., [4], have assumed Rayleigh fading because it is both conservative and quite prevalent.

The case of fixed wireless paths, e.g., for wireless multipoint communication systems, is different. Here, there can still be multipath echoes, and the complex sums of received waves still vary over space and frequency. However, with both ends of the link fixed, there will be—to first order—no *temporal* variations. What alters this first-order picture is the slow motion of scatterers along the path, e.g., pedestrians, vehicles, and wind-blown leaves and foliage. As a result, the path gain at any given frequency will exhibit slow temporal variations as

Manuscript received June 26, 2008; revised December 18, 2008. The review of this paper was coordinated by Dr. K. T. Wong.

L. J. Greenstein is with the Wireless Information Network Laboratory, Rutgers University, North Brunswick, NJ 08902 USA (e-mail: ljg@winlab.rutgers.edu).

S. S. Ghassemzadeh is with the Communication Technology Research Department, AT&T Labs-Research, Florham Park, NJ 07932 USA (e-mail: saeedg@research.att.com).

V. Erceg is with the Broadcom Corporation, San Diego, CA 92128 USA (e-mail: verceg@broadcom.com).

D. G. Michelson is with the Radio Science Laboratory, Department of Electrical and Computer Engineering, University of British Columbia, Vancouver, BC V6T 1Z4, Canada (e-mail: davem@ece.ubc.ca).

Color versions of one or more of the figures in this paper are available online at http://ieeexplore.ieee.org.

Digital Object Identifier 10.1109/TVT.2009.2018549

the relative phases of arriving echoes change. Because these perturbations are often slight, the condition of a dominant fixed component plus a smaller fluctuating component takes on a higher probability than that for mobile links. Furthermore, since temporal perturbations can occur on *many* scatter paths, the convergence of their sum to a complex Gaussian process is plausible. Therefore, we can expect a Ricean distribution for the gain magnitude, with a higher K-factor, in general, than that for mobile cellular channels.

During the past decade, numerous studies have aimed to reveal various aspects of the manner in which fixed wireless channels fade on non-line-of-sight paths typical of those encountered in urban and suburban environments [5]–[12]. One set of researchers has focused on determining the manner in which wind blowing through foliage affects the depth of fading on fixed links, e.g., [6]–[9], while another has focused on scenarios in which relatively little foliage is present but scattering from vehicular traffic presents a significant impairment, e.g., [10]–[12].

In this paper, we focus on the development of statistical models that capture the manner in which fading on fixed wireless channels in suburban macrocell environments depends upon the local environment, the season (leaves or no leaves), the distance between the base and the remote terminal, and the height and beamwidth of the terminal antenna. We do so using an extensive body of data collected during four distinct experiments. Our earlier findings were presented in [13] and were ultimately adopted by IEEE 802.16 [14]. Here, we fill in the essential detail concerning the measurement campaigns and present plausible physical arguments to explain our observations. Furthermore, we demonstrate that the variability of the channel about the median can be divided into a component due to variation at a fixed location and another due to variation between locations. Finally, we present what we believe are the first observations of simultaneous fading events on different links within the same suburban macrocell.

In Section II, we review a method for computing K from time records of path gain magnitude that is particularly fast and robust and therefore suited to high-volume data reductions. We show that it is also highly accurate. In Section III, we describe several experiments that were conducted at 1.9 GHz to measure path gains on fixed wireless links. The data from these experiments were used to compute K-factors for narrow-band channels. In Section IV, we show how the computed results were used to model the statistics of K as a function of various parameters. We also examine such issues as the variability of K with time, frequency, and location and the influence of wind conditions on K. Section V concludes the paper.

II. Estimation of Ricean K-Factor

A. Background

Our practical objective is to model narrow-band fading by means of a Ricean distribution over the duration of a fixed wireless connection. We assume that the duration of a connection is in the 5–15-min range, and we will compute K for finite time intervals of that order. Later, we will show how K can vary with the time segment and with frequency. We will also show that the statistical model for K is very similar for 5- and 15-min intervals.

B. Formulation

We characterize the complex path gain of the narrow-band wireless channel by a frequency-flat time-varying response

$$g(t) = V + v(t) \tag{1}$$

where V is a fixed complex value, and $v(t)$ is a complex zero-mean random time fluctuation caused by vehicular motion, wind-blown foliage, etc., with variance σ^2. This description applies to a particular frequency and time segment. Both V and σ^2 may change from one time–frequency segment to another.

We assume that the quantity actually measured is the received narrow-band power, which, suitably normalized, yields the instantaneous power gain

$$G(t) = |g(t)|^2 . \tag{2}$$

Various methods have been reported to estimate K using moments calculated from time series such as (2), e.g., [15]–[17].

We can relate K to two moments that can be estimated from the data record for $G(t)$. The first moment G_m is the average power gain; its true value (as distinct from the estimate

$$G_m = \sum_{i=1}^{N} \frac{G_i}{n} \tag{3}$$

computed from finite data) is shown in [15] to be

$$G_m = |V|^2 + \sigma^2. \tag{4}$$

The second moment G_v is the RMS fluctuation of G about G_m. The *true* value of this moment (as distinct from the estimate

$$G_v = \sqrt{\frac{1}{N}\sum_{i=1}^{N}(G_i - G_m)^2} \tag{5}$$

calculated from finite data) is shown in [15] to be

$$G_m = \sqrt{\sigma^4 + 2|V|^2\sigma^2}. \tag{6}$$

In each of (4) and (6), the left-hand side can be estimated from the data, and the right-hand side is a function of the two intermediate quantities we seek. Combining these equations, we can solve for $|V|^2$ and σ^2, yielding

$$|V|^2 = \sqrt{G_m^2 - G_v^2} \tag{7}$$

$$\sigma^2 = G_m - \sqrt{G_m^2 - G_v^2}. \tag{8}$$

Finally, K is obtained by substituting these two values into

$$K = |V|^2/\sigma^2. \tag{9}$$

Note that σ^2 as defined here is twice the RF power of the fluctuating term, which is why the customary factor of two

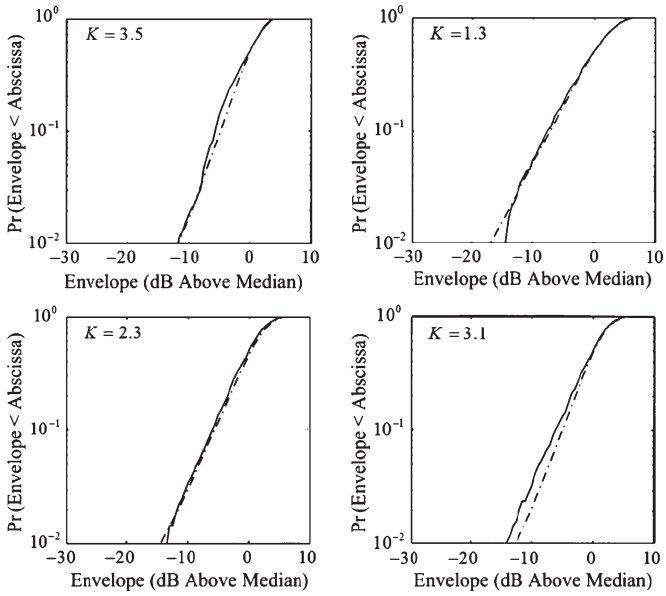

Fig. 1. Four typical envelope cdf's, comparing actual data (solid curves) with Ricean distributions (dashed curves). The latter use K-factors derived from data via the moment method.

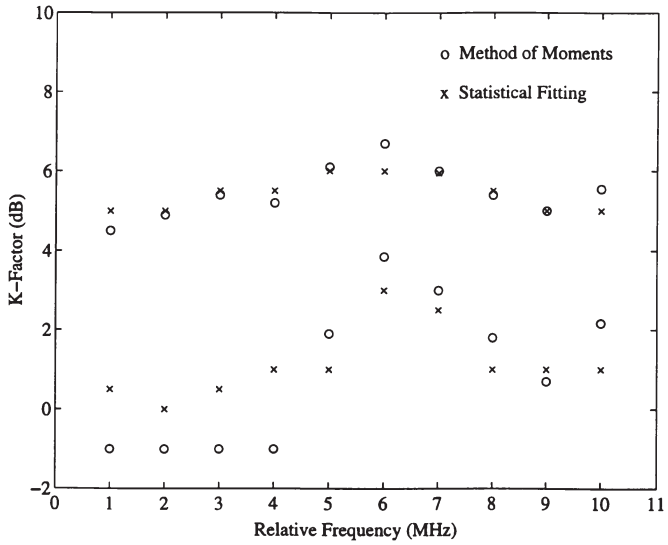

Fig. 2. Comparisons, for each of two locations, of K versus f, where K is derived via two methods: the moment method and the least-mean-square fitting of empirical and Ricean distributions. These results are typical and show that the moment method predicts K to within 2 dB (usually much less) of the results for least-mean-square fitting.

(see [3, eq. (5.60)]) is not present in (9). The K-factor and average power gain G_m jointly determine the Ricean envelope distribution.

The choice of the measurement interval is a necessary compromise between obtaining a large sample size and preserving the stationarity within the interval. Given the rate at which meteorological conditions, particularly wind conditions, usually change, we considered 15 min to be suitably small. This supposition is supported by the consistency of our results for 5- and 15-min segments.

C. Validation

For each of several fixed wireless paths located in suburban New Jersey, we collected 5-min time sequences of received power at 1.9 GHz (see Section III). For each path, we can compute a cumulative distribution function (cdf) of the measured samples. This is the empirical cdf of the received envelope. We can also estimate G_m and K, the two parameters that define a Ricean distribution, and then compute a Ricean distribution that should closely match the empirical one.

Comparisons for four typical cases are shown in Fig. 1. Each corresponds to a particular time, frequency, and transmit–receive path. In each case, the results show that, although some cases fit better than others, the Ricean distribution obtained using the estimated moments is quite close to the empirical one. Deviation from the ideal can usually be interpreted as the result of a transient fading event affecting the distribution of either the fixed or scatter component. In the absence of more detailed information, e.g., time- and/or angle-of-arrival data, it is difficult to offer further interpretation of a given result.

We also examined goodness-of-fit methods to determine K. Although they are accurate, they are also much more time intensive and, thus, not conducive to the reduction of large quantities of data [1]. Moreover, they produce results not much different from those using the moment method. Fig. 2 gives two typical comparisons, based upon data collected in suburban New Jersey, in each of which K-factors at different frequencies over a 9-MHz bandwidth are shown for both the moment method and the goodness-of-fit method. The latter consisted of matching the data-derived cdf of G to a Ricean one, with K chosen to minimize the RMS decibel difference between cdf's over the probability range from 1% to 50%.

We note that, if the calculated moment G_v exceeds the calculated moment G_m, the calculated result for $|V|^2$, from (7), will be imaginary. When this happens, it is because either 1) the underlying process is not well modeled as Ricean, or 2) the statistical noise of the finite time record produces a G_v slightly larger than G_m instead of being equal to or slightly smaller than G_m.

In our reductions, we declare K to be 0.1 if G_v exceeds G_m by less than 0.5 dB[1]; if it is larger than that, we remove the particular record from the database. In our reductions of 5-min records, such removals occurred in a small fraction of all cases (less than 2%). In our reductions of 15-min records, the fraction was even smaller.

Typical 5-min records of received decibel power are shown in Fig. 3. Such records, converted to linear power and suitably normalized, yield records of $G(t)$, as given in (2). Our examination of data like these indicate that relatively shallow fluctuations, on a time scale of 1 or 2 s, occur on most links, in addition to possibly deeper fluctuations on a time scale of tens of seconds [18].

D. Properties of the Ricean K-Factor

The complex fluctuation $v(t)$, from (1), for a given frequency is due to temporal variations in gain on one or more paths. If these variations are independent among paths, then the

[1]Over the range below 0.1, the precise value of K is immaterial. For all practical system purposes, it is zero, but we assign it a value 0.1 (-10 dB) for convenience in tabulating statistics.

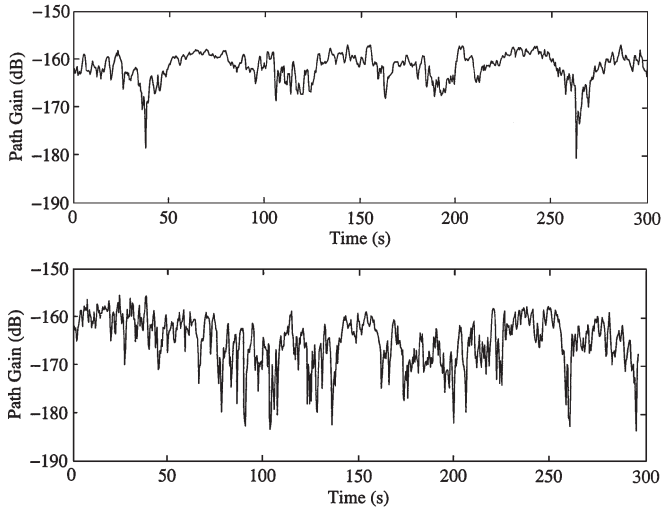

Fig. 3. Two typical examples of measured path gain at a particular frequency over 280 s. Note that fading can be quite deep and that temporal fluctuation rates are on a scale of hertz or lower.

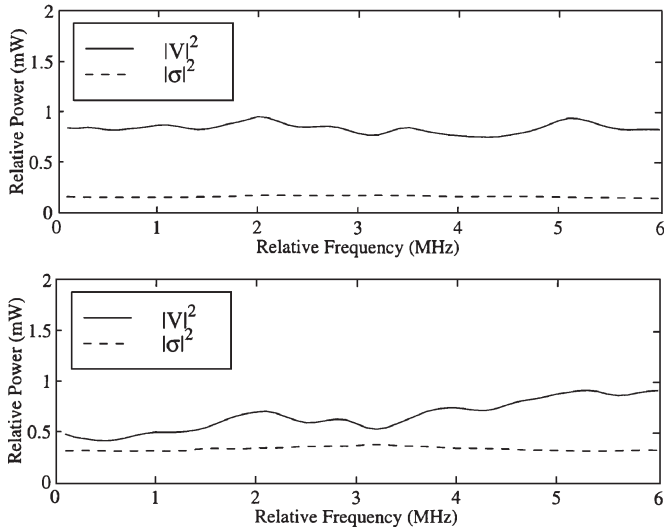

Fig. 4. Two typical examples of the fixed and mean-square "scatter" components of path gain, as functions of frequency. Note that σ^2 is fairly flat with frequency, so that the frequency variation of $K = |V|^2/\sigma^2$ follows that of $|V|^2$.

mean-square value of $v(t)$ will be flat with frequency. [To see this, write $v(t)$ as the response at a given frequency to a sum of delayed echoes, where the echoes have time-varying independent gains of zero mean. Next, derive the ensemble mean of $|v(t)|^2$, and note that it is independent of the given frequency.] This result is observed in the sample plots, in Fig. 4, of $|V|^2$ and σ^2 versus frequency. These plots are typical of what we observe on most links, i.e., σ^2 exhibits a relative flatness with frequency, with the small perturbations being attributable to statistical effects. Since K is the ratio of $|V|^2$ to σ^2, we conclude that its variation with frequency is essentially proportional to that of the fixed gain component. This, in turn, depends on the complex amplitude versus delay of the significant echoes, which varies from one transmit–receive path to another [19].

Other properties of the Ricean K-factor can be anticipated by similar reasoning.

1) At a given distance, we might suppose that the strength of the scatter component, which is the result of rays coming from a multiplicity of directions, will vary far less than the strength of the fixed component, which is dominated by rays coming from the direction of the base station and which will be strongly affected by local shadowing along that direction. Thus, we expect K to exhibit lognormal statistics across locations, with a standard deviation comparable to that associated with shadow fading.
2) By definition, remote terminals in macrocell environments generally lie in the shadow region of the obstacles that block its line of sight to the base station. As the height of the terminal antenna increases, the diffraction angle will decrease, and the strength of the fixed component will increase. Again, we might suppose that the scatter component, which is the result of reflection and scattering from a multiplicity of directions, will vary far less with the terminal height than the fixed component. Thus, we expect K to increase with the terminal height.
3) Because the scattered component will come from all other directions, increasingly less of the scatter signal will be received as the beamwidth of the receiving antenna decreases. Thus, we expect K to increase as the antenna beamwidth decreases.
4) Previous work has shown that the average wind velocity above treetop level does not vary much over distances of several kilometers [20]. Thus, we expect that fading events associated with windblown foliage should be fairly well correlated between links within a typical cell.

In the next section, we describe the experiments that we conducted to investigate the validity of these and other conjectures.

III. Measurement Program

The database used in our modeling comes from four distinct experiments conducted in suburban areas, as summarized in Table I. Each of the four experiments has its own purposes, strengths, and limitations but had, as one of its objectives, the determination of K-factors on fixed wireless paths. Collectively, this set has provided an extensive body of data from which Ricean K-factors can be computed and modeled. We describe the four experiments in this section and report the K-factors reduced from them in the next section. It should be noted that fading on the uplink and downlink are reciprocal for the same path and frequency and that all the measurements reported here were for the downlink only. Furthermore, all measurements were made using an equipment van parked on the street, with the terminal antenna pointed to receive the maximum downlink signal. All of our data were collected in quiet residential neighborhoods with minimum residential and pedestrian traffic.

We characterized each neighborhood according to the general nature of both the terrain and the trees and foliage but did not attempt to characterize vegetation density or building-to-lot area ratios along individual paths. Whereas such an approach was used in [21] to assist in the prediction of mean path loss in urban environments, our measurement database, large as it is, is insufficient to take full advantage of such detail.

TABLE I
SUMMARY OF THE FOUR EXPERIMENTS

Exp. No.	Measurement parameters	Measurement Duration	Terminal Antenna	Geography, Seasons	Uses for Reduced Data
1	9 MHz (90 frequencies) Base Antenna: Single-pol Panel h=15 and 30m	5-minute samples at each downlink location.	Single-pol; b = 17°, 30°, 65°; h = 3 m, 10 m	Three transmit sites in NJ. Tens of downlink locations for each site. Summer and Winter.	Devise first-order model for pdf of K at any time, frequency and location in NJ suburban environments.
2	CW (one frequency) Base Antenna: Single-pol Omni-directional h=25m	5-minute samples at each downlink location.	Single-pol; b = 45° and omni antenna; h = 3 m	One transmit site in WA, two in IL. Tens of downlink locations for each site. Summer only	Reinforce first-order model. Examine regional differences. Show effects of omni vs. directional antennas.
3	6 MHz (60 frequencies) Base Antenna: Single-pol Panel h=15 and 30m	Long runs (12 – 24 hrs) at each downlink location.	Dual-pol; b = 32°; h = 3 m	Two transmit sites in NJ. Seven and nine downlink sites. Summer only.	Reinforce first-order model. Examine variations with time and frequency.
4	CW (one frequency) Base Antenna: Single-pol Omni-directional h=25m	Long runs (2 – 12 hrs) at each downlink location.	Dual-pol; b = 32°; h = 3 m	Two transmit sites in IL. 14 and 21 downlink locations. Summer only.	Reinforce first-order model. Examine regional differences. Examine variations with time.

A. *Experiment 1: Short-Term Measurements in New Jersey*

Downlink measurements were made for three transmit sites in northern and central New Jersey. For each site, data were collected at 33 or more downlink locations during summer (trees in full bloom), and repeat measurements were made at half or more of these locations during winter (trees bare). Distances ranged (more or less uniformly) from 0.5 to 9 km. This was the major experiment in our study, and so, we summarize a number of its features in Table II.

The transmit sites were located in the residential communities of Holmdel, Whippany, and Clark. Each site overlooked a terrain consisting of rolling hills with moderate to heavy tree densities and dwellings of one or two stories. Furthermore, each site used a panel-type transmitting antenna with elevation and azimuth beamwidths of 16° and 65°, respectively. The antenna was fed by a 10-MHz swept frequency generator centered at 1985 MHz.

For each downlink location (i.e., receive terminal site) for each of two antennas at each of two heights (3 and 10 m), the data record consists of 700 "snapshots" of received power versus frequency. The receiver was a swept frequency spectrum analyzer equipped with a low noise amplifier to increase its sensitivity; its sweep was synchronized to that of the transmitter using the 1-pulse-per-second signal from a GPS receiver. The unit was operated in sample detection mode to enhance its ability to characterize the first-order statistics of random signals. A local controller handled the configuration, operation, and data acquisition. The "snapshots" for each antenna/height combination are spaced by 0.4 s, for a total time span of nearly 5 min, and each consists of 90 samples, spaced by 100 kHz, for a frequency span of 9 MHz. In the data processing, the power samples, which were recorded in decibels of the measured power referenced to 1 mW (dBm), were calibrated and converted to linear path gain.

TABLE II
FEATURES OF EXPERIMENT 1

Transmit Site (Location, Antenna Height)	Terrain	Number of Downlink Locations	Terminal Antenna (Azimuth Beamwidth, Height)
Holmdel, 15 m	Rolling hills, moderate-to-heavy tree density with some close-in tree blockage, 1 – 2 story dwellings within the transmitting sector.	44 Summer, 44 Winter	Dish; b = 17° Panel; b = 65° h = 3 m and 10 m
Clark, 15 m	Rolling hills, moderate-to-heavy tree density, 1 – 2 story dwellings and some commercial buildings within the transmitting sector.	33 Summer, 14 Winter	Two panel antennas, spaced by 1.8 m; b = 30° h = 3 m and 10 m
Whippany, 30 m	Rolling hills, moderate-to-heavy tree density, 1 – 2 story dwellings within the transmitting sector.	37, Summer, 20 Winter	Two panel antennas, spaced by 1.8 m; b = 30° h = 3 m and 10 m

B. Experiment 2: Short-Term Measurements in Illinois and Washington

During the spring and summer, measurements were made in the vicinity of a transmit site in Washington (Redmond, near Seattle) and from two transmit sites in Illinois (Bellwood and Naperville, near Chicago). The number of downlink locations was more than 100 for each transmit site at distances ranging from 0.4 to 2.2 km.

All three transmit sites were in suburban/residential environments. The Redmond site overlooked a hilly terrain with heavy tree cover. The Bellwood and Naperville sites overlooked an extremely flat terrain with high and low tree densities, respectively. The measurement data were collected using a continuous-wave (CW) transmitter and multichannel narrowband measurement receiver manufactured by Grayson Electronics. The amplitude resolution was 1 dB, which was deemed to be adequate for the purpose of determining K.

Two antennas were used at each downlink location: one directional and one omnidirectional. They were used to simultaneously make measurements and were both mounted at a height of 3 m. No measurements were made in winter. Each measurement consisted of recording the received signal power at a rate of 400 samples/s for 5 min.

C. Experiment 3: Long-Term Measurements in New Jersey

Long-term measurements (record lengths of up to 24 h) were made from two transmit sites in northern New Jersey: one in Iselin and one in Whippany. The Whippany site was the same as the one used in Experiment 1. The Iselin site used a similar transmit antenna, at a height of 15 m, and overlooked a residential area similar to that in Whippany. The total number of downlink locations processed for these two sites was 16, with distances ranging from 0.5 to 3.1 km.

The measurement approach was similar to that for Experiment 1: The received power was recorded at 100 frequencies over 10 MHz centered on 1985 MHz. The three main differences were 1) the reception was on the two branches of a slant-45° dual-polarized antenna with an azimuth beamwidth of 32°, 2) data were recorded for continuous intervals ranging from 11 to 24 h, and 3) the wind speed was continuously measured and recorded at both ends of the path.

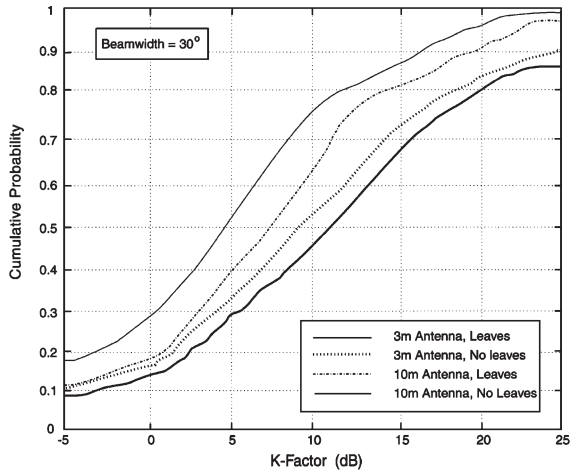

Fig. 5. CDFs of the K-factor for an antenna beamwidth of 30°. These results are for New Jersey locations measured in Experiment 1.

In the data reductions, only the central 6 MHz of data were processed (60 frequencies), and the long time records were parsed into 15-min segments. Thus, a 24-h recording produced a 96 × 60 matrix of time–frequency segments, and K was computed for each one. This permitted us to obtain K for time segments longer than the original 5-min samples as well as to examine slow variations in K over the course of a day. The decision to limit the number of frequencies processed was a business decision that does not materially affect the results. Indeed, the fact that single-carrier and multicarrier results with different parameters yield consistent results gives us greater confidence in the generality of our findings.

D. Experiment 4: Long-Term Measurements in Illinois

Long-term measurements were made from two transmit sites in Illinois, i.e., the same Bellwood and Naperville sites used in

TABLE III
MEDIAN K-FACTORS FOR EXPERIMENT 1*

Antenna Beamwidth, b	Summer (Leaves)		Winter (No Leaves)	
	h = 3 m	h = 10 m	h = 3 m	h = 10 m
17°	6.0 dB	8.0 dB	10.0 dB	12.5 dB
30°	4.5 dB	7.5 dB	9.0 dB	11.0 dB
65°	2.5 dB	5.0 dB	6.0 dB	8.5 dB

* All values have been rounded to the nearest 0.5 dB.

Experiment 2. For Bellwood, there were 14 downlink locations, at distances ranging from 0.35 to 1.4 km; for Naperville, there were 21 downlink sites, at distances ranging from 0.6 to 2.1 km.

The measurement approach was similar to that of Experiment 2, with differences similar to those between Experiments 1 and 3: 1) the use of dual-polarized slant-45° antennas with 32° beamwidths; 2) the long-term data records, with measurements ranging from 2 to 12 h; and 3) the measurement and recording of wind speed.

IV. RESULTS

A. First-Order Statistical Model for K

General: By a "first-order statistical model," we mean one that gives the probability distribution of K, given a set of path and system parameters, e.g., distance, season, terminal antenna height, and terminal antenna beamwidth, based upon measurements collected over time, frequency (in the case of multicarrier signals), and location. A "second-order statistical model" would, in addition, sort out the individual variations with time, frequency, and location. We provide some results on that aspect in Section IV-C.

The model we present here is entirely based on the database for Experiment 1, which is the richest in terms of parameter variation. However, we will expand this model and confirm its validity by using results from the other three experiments.

Database: Each short-term measurement in New Jersey initially produced 750 "snapshots," spaced by 0.4 s, of received power versus frequency at 100 frequencies spaced by 100 kHz. For convenience in the data reductions, however, each record was trimmed to 700 "snapshots" (280-s time span) and 90 frequencies (9-MHz frequency span). We thus computed 90 K-factors, each using recorded power versus time over 4.67 min. In only 1% of all cases did the method in Section II fail to produce a real solution for K.

K-Factor Medians: As noted in Table I, the database encompasses two seasons [summer (leaves) and winter (no leaves)], two antenna heights (3 and 10 m), and three antenna beamwidths (17°, 30°, and 65°), for a total of 12 combinations. For each parameter set (season, height, and beamwidth), we computed K over a large population of frequencies and locations and then computed a cdf. One such result is shown in Fig. 5, which shows four cases (2 seasons $\times$ 2 heights) for a given beamwidth. To compress the information in curves like this, we extracted the median K for all the cdf's and analyzed the 12 values. These values are summarized in Table III, rounded to the nearest 0.5 dB.

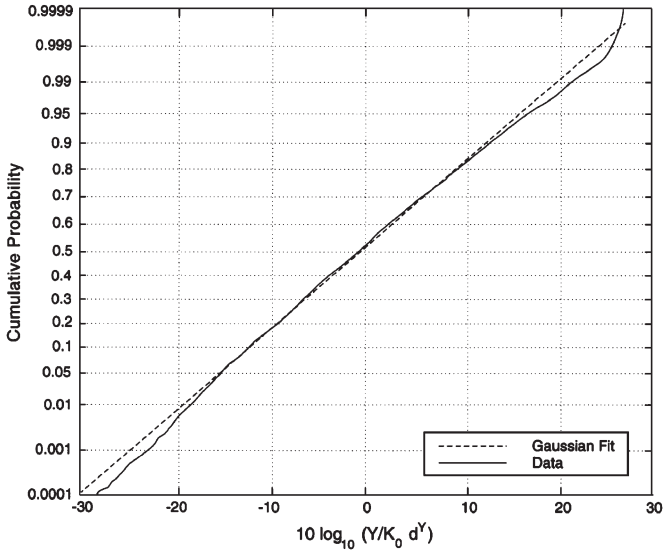

Fig. 6. CDF of the K-factor variation about the distance regression line for the data of Experiment 1. The closeness to a straight line on this scale implies a near-lognormal distribution. The slope implies a standard deviation of 8 dB.

Methodology: First, we examine the influence of season (leaves versus no leaves). For the six combinations of two antenna heights and three antenna beamwidths, we see a consistent increase in median K from summer to winter, ranging from 3.5 to 4.5 dB with an average close to 4.0 dB (or 2.5 in linear units). We attribute the increase to the reduction in gain variations when there are no windblown leaves.

Second, we examine the influence of antenna height h. For the two seasons and three beamwidths, we see a consistent increase from 3 to 10 m, ranging from 2.0 to 3.0 dB with an average of 2.4 dB. If we assume a power-law relationship, i.e., $K \propto h^{\alpha}$, then $\alpha = 0.46$. This modest increase with h is consistent with intuition: we expect there to be a gradual increase in line-of-sight power (which is generally fixed in time) as the terminal antenna height increases. In hindsight, it would have been preferable to collect data at three heights rather than just two. On the other hand, such trends, particularly over a limited range of values as in this case, are almost always approximately linear on a log–log plot, indicating a power-law relationship. It is unlikely that the true decibel values for

TABLE IV
SUMMARY OF RESULTS FOR EXPERIMENT 2

Antenna	Site	Distance Exponent, γ	1 km Intercept, K_1 (dB)	σ(dB)
	Naperville, IL	-0.35	5.6	5.3
Omni-directional	Bellwood, IL	-0.20	1.9	4.1
	Redmond, WA	-0.42	5.5	5.6
	Naperville, IL	-0.52	12.3	5.2
Directional	Bellwood, IL	-0.30	8.0	3.4
	Redmond, WA	-0.12	11.6	6.4

heights in between would seriously be different from what the power-law relationship predicts. Because the behavior of K with height will change as the terminal antenna rises out of the local clutter, care should be taken not to extrapolate beyond the height of the clutter.

Third, we examine the influence of antenna beamwidth b. In the Holmdel measurements, beamwidths of 17° and 65° were used in simultaneous measurements. The difference in median K between these two beamwidths ranges from 3.0 to 4.0 dB, with an average of about 3.6 dB. If we assume a power-law relationship, i.e., $K \propto b^{\beta}$, then $\beta = -0.62$. When we apply this law to the medians for $b = 30°$, which were collected elsewhere (Clark and Whippany), the agreement is within 1 dB.

The result for β is particularly satisfying. If there was no angular scatter, we would expect to see $\beta = 0$ (K-factor unaffected by beamwidth), and if the scatter were uniform in strength over 360° in azimuth, we would expect to see $\beta = -1.0$ (K-factor directly proportional to antenna gain). The value $\beta = -0.62$ is consistent with an environment of significant but not totally uniform scatter.

Finally, we consider the influence of distance d. If we assume a power-law relationship, i.e., $K \propto d^{\gamma}$, then the aforementioned results lead us to the formulation

$$K \cong F_s F_h F_b K_o d^{\gamma} \ (d \text{ in kilometers}) \tag{10}$$

where the factors are defined as follows.

1) F_s is the seasonal factor

$$F_s = \begin{cases} 1.0, & \text{Summer (Leaves)} \\ 2.5; & \text{Winter (No Leaves).} \end{cases} \tag{11}$$

2) F_h is the height factor

$$F_h = (h/3)^{0.46} \ (h \text{ in meters}). \tag{12}$$

3) F_b is the beamwidth factor

$$F_b = (b/17)^{-0.62} \ (b \text{ in degrees}). \tag{13}$$

K_o and γ are constants to be optimized via regression fitting. Now, we form the data variable

$$Y = K/(F_s F_h F_b) \cong K_o d^{\gamma}. \tag{14}$$

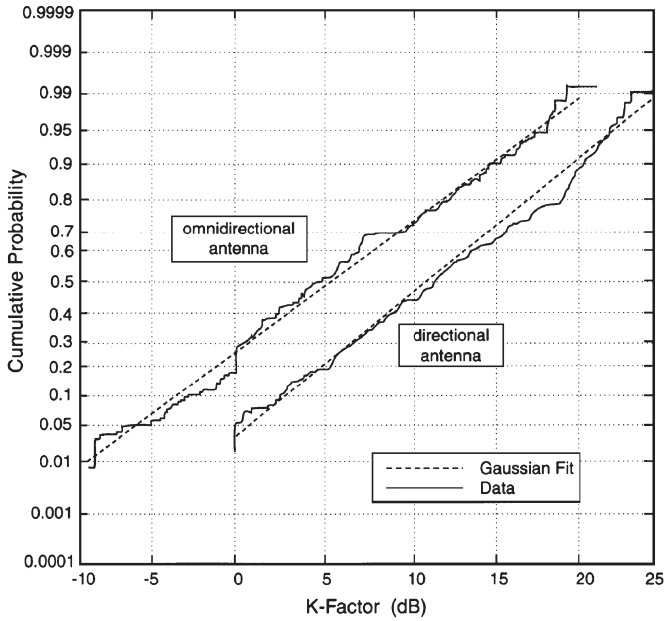

Fig. 7. CDFs of the K-factors computed for Naperville, IL, in Experiment 2. Both results show near-lognormal distributions. The standard deviation is similar for each (slightly above 6 dB), but the median for the directional antenna is roughly 6 dB higher than that for the omnidirectional antenna.

For every K computed in the database, there is an associated season, height, beamwidth, and distance, and so, a Y value can be computed and paired with d. We can then perform a regression fit between Y and d over the database.[2]

The result we get is that $K_o \cong 10.0$ dB and $\gamma \cong -0.5$ dB. The standard deviation of 10 log Y about the regression curve is just under 8.0 dB. Moreover, the distribution of 10 log Y about that curve is very nearly Gaussian, as seen in Fig. 6. The meaning is that K can be very accurately modeled as a lognormal variable, with a median value easily related to path and system parameters.

Summary of the First-Order Model: At any time, frequency, and location, the K-factor in a given season, for a given antenna

[2]We are implicitly assuming a common distance dependence for all parameter combination, which is an assumption not fully vindicated by the data. We will see that the price for this simplification is a modest increase in variability about the median.

TABLE V
SUMMARY OF RESULTS FOR EXPERIMENT 4

Distance	Site	Median K (dB)		σ (dB)	
		Branch 1	**Branch 2**	**Branch 1**	**Branch 2**
$d < 1$ km	Naperville, IL	16.7	16.6	4.6	3.5
	Bellwood, IL	14.9	14.6	3.4	3.1
$d \geq 1$ km	Naperville, IL	17.9	17.6	6.2	4.8
	Bellwood, IL	14.8	13.4	5.3	6.1

height, antenna beamwidth, and distance, can be described as follows in a suburban New Jersey type of terrain:

$$K = K_1 d^{\gamma} u \tag{15}$$

where K_1 is the 1-km intercept

$$K_1 = F_s \cdot F_h \cdot F_b \cdot K_o \tag{16}$$

$K_o \cong 10.0$ dB; $\gamma \cong -0.5$; F_s, F_h, and F_b are given by (9)–(11); and u is a lognormal variate, whose decibel value is zero mean with a standard deviation σ of 8.0 dB.

We observe that, for each of the 12 parameter sets identified earlier, the standard deviation about the decibel median for that set was about 7 dB, or a bit more. The increase of less than 1 dB in σ is mostly due to simplifications in modeling the median, including assuming a common distance dependence for all parameter sets. This small degree of added variability is a minor price for obtaining a simple and user-friendly model.

B. Consistency Checks

The reduced results from Experiment 2 are summarized in Table IV. In computing K via (1)–(9), the percentage of data removed because K was not real was 0%, 1%, and 2% for Redmond, Naperville, and Bellwood, respectively, with no difference between omnidirectional and directional antennas. We make the following observations.

1) The main difference between the terrains in Bellwood and Naperville is tree density (high in Bellwood and low in Naperville). The roughly 4-dB higher values for K_1 in Naperville (3.7 and 4.3 dB for omnidirectional and directional antennas, respectively) match the seasonal difference for New Jersey (leaves versus no leaves).
2) The higher values of K_1 for the directional antennas closely follow the beamwidth dependence given by (13), which predicts a 5.6-dB increase for the 45° beamwidth used in Illinois and a 6.7-dB increase for the 30° beamwidth used in Washington. The agreements (within 1 dB) are exceptionally good, particularly since (13) was empirically derived for beamwidths of 65° and below.
3) The values of K_1 for Bellwood and Naperville (taking proper account of the beamwidth and season) are within 0.5 dB of the values predicted by the first-order model.
4) The numerical values for γ and σ in Table IV are consistent with those for the first-order model. The distance exponent is smaller in some cases, and so is the standard deviation. However, the data volume for Experiment 2 is not large enough for these differences to be statistically significant. What the tabulations show that is significant is that σ does not change with antenna beamwidth, in agreement with the first-order model.
5) The cdf's of K in Illinois and Washington show the same lognormal character predicted by the first-order model. For example, Fig. 7 shows cdf's of K, for both antenna types, in Bellwood.

Now, moving to Experiment 3, we present a result that shows a remarkable consistency with the first-order model: Over 60 frequencies and up to 96 time segments at 16 locations, K was found to be essentially lognormal, with a median and standard deviation of 8.5 and 7.1 dB, respectively. Since these data were for distances uniformly clustered between 0.5 and 2.0 km, the median closely corresponds to the 1-km intercept of the model, i.e., K_1 in (16). For the conditions summer, $h = 3$ m, and $b = 32°$, the model predicts K_1 to be 8.3 dB. Furthermore, the 7.1-dB standard deviation is close to the 8.0-dB model value, which is slightly elevated due to modeling approximations.

Note that Experiments 1 and 3 were conducted on different paths, in different years, using two different measurement intervals (5 and 15 min) and different antenna types. Given all that, the agreement in the global statistics of K is indeed remarkable.

Somewhat less affirming is a comparison with the results from Experiment 4, summarized in Table V. On the positive side, these results repeat the increase in median K-factor at Naperville relative to Bellwood (an average of about 2.7 dB). On the other hand, the median K-factors for both sites are several decibels higher than those predicted by the model (an average increase of about 6 dB), and the standard deviations are 1–3 dB lower. A plausible explanation is the lower tree densities, for *both* sites, relative to those in New Jersey. If the wind-induced motion of trees (branches and leaves) is a significant cause of path gain variations, then we should expect to see tree density as a separate determinant of the K-factor. The comparisons here between the Illinois and New Jersey data may be a step toward establishing such a correspondence.

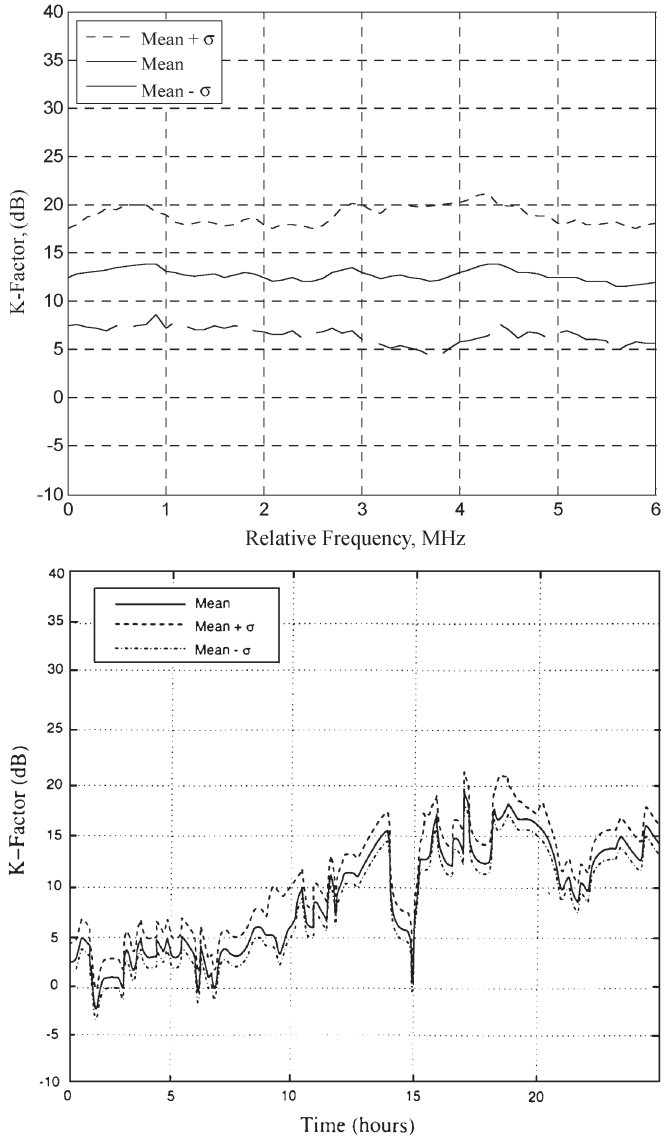

Fig. 8. Variation of K with (top) frequency and (bottom) time. The results shown are for a typical path. The standard deviation (σ) for the top graph is computed over 96 15-min intervals at each frequency; for the bottom graph, it is computed over 60 frequencies in each 15-min time interval. Note the relative constancy of the results with frequency but not time.

C. Variations With Time, Frequency, and Location

The variation of K with time at a given frequency is due to slow changes of various kinds, e.g., changes in physical objects within the environment and wind conditions. (Temperature and humidity have a significant effect on long-distance point-to-point links because they affect both the refractive index profile and the atmospheric turbulence; their possible role in impairing non-line-of-sight fixed wireless systems is an area for further study.) The variation in K with frequency at a given time is due to a multipath, which causes frequency-selective variations in the RF gain. Taken together, the time/frequency variations at a given location account for a significant part of the K-factor variability reflected in the first-order model.

However, another significant component is the variation among locations. For analysts doing system simulations, it is important to separate the two kinds of variability, as their impacts are different. We can do this separation by expressing the decibel value of u, from (15), as

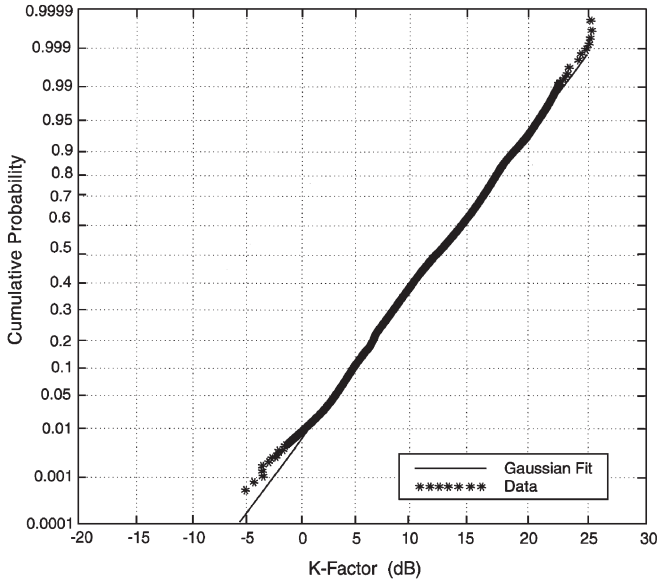

Fig. 9. CDF of K for a given location, computed over 96 15-min intervals at each of the 60 frequencies. For this typical case, the variation of K with time and frequency at a given location is seen to be essentially lognormal.

$$10 \log u \equiv U_{\mathrm{TF}} + U_{\mathrm{LOC}} \tag{17}$$

where U_{TF} and U_{LOC} are independent zero-mean Gaussian variates with standard deviations of σ_{TF} and σ_{LOC}, respectively. U_{TF} varies at a given location as a function of time of connection and frequency assignment; U_{LOC} is fixed at a given location but varies among locations over the terrain. The RMS sum of the two standard deviations is σ in the first-order model.

To make these points more concrete, Fig. 8 (top) shows the variability of the decibel K-factor for a particular New Jersey path over 6 MHz and 24 h. This plot conveys the median and standard deviation of K, computed over a 24-h period, i.e., over 96 15-min segments, as a function of frequency. Note that the variability at any given frequency can be severe, e.g., the $\pm\sigma$ region can span a range from 4 to 21 dB. Furthermore, there is roughly uniform behavior with respect to frequency, i.e., there are no "preferred" frequencies at the chosen location. This general observation applies to other locations as well.

Another version of the same data [Fig. 8 (bottom)] conveys the median and standard deviation, computed over 6 MHz, i.e., over 60 frequencies, as a function of time. Here, the spread in frequency at a given time is small. This spread depends on the delay profile of the channel and can significantly vary from one location to another, as we have observed [19]. Furthermore, there can be "good" time periods (high K) and "bad" time periods (low K), as we see in this example.

The variability of K over time and frequency was evaluated for each of the 16 downlink locations in the database of Experiment 3. First, we found that the variability is well described as lognormal, as exemplified in Fig. 9. Second, the standard deviation of K per location had an average value of 5.7 dB, with a fairly narrow spread across the 16 locations. The median of K per location had a standard deviation across locations of

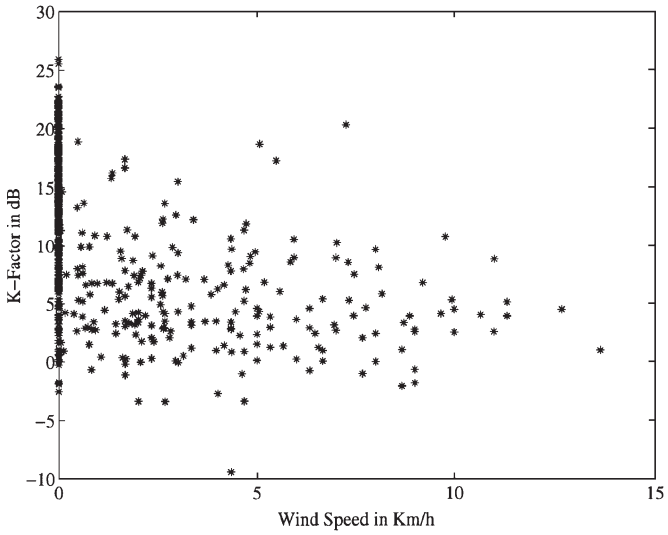

Fig. 10. Scatter plot of K-factor and wind speed for six New Jersey locations.

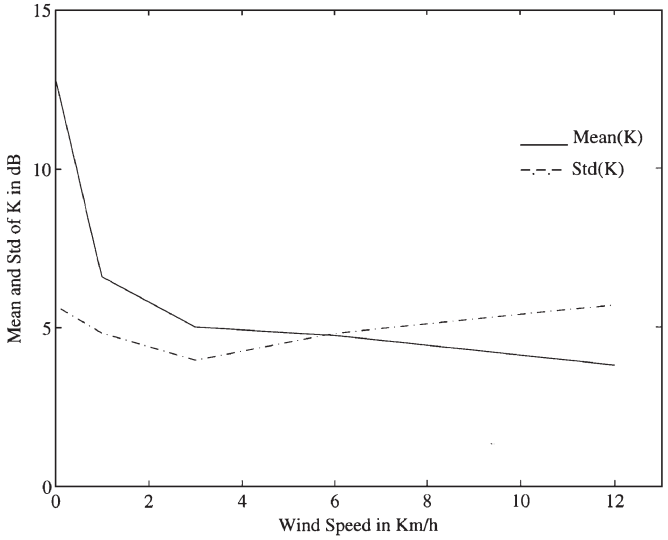

Fig. 11. Mean and standard deviation of the decibel K-factor as functions of wind speed for the six New Jersey locations. The general inverse relationship of K and wind speed is evident.

4.3 dB. The RMS sum of the two standard deviations is 7.1 dB, which we cited earlier as the global value over time, frequency, and location.

We propose that, in the lognormal model for K, 10 log u should be decomposed as in (17), with $\sigma_{\mathrm{TF}} = 5.7$ dB and $\sigma_{\mathrm{LOC}} = 5.6$ dB, the latter being larger than 4.3 dB to reflect our imperfect modeling of the median K (see Section IV-A). The RMS sum of the two σ's is 8.0 dB.

D. Influence of Wind Conditions

In the long-duration path-loss measurements of Experiments 3 and 4, we simultaneously measured wind speed at the base and terminal locations. The wind speed data were recorded every second and later averaged, in offline processing, over 15-min intervals. Here, we present some illustrative results based on 24-h records for each of the six New Jersey locations (a data subset of Experiment 3) and a single 48-h record

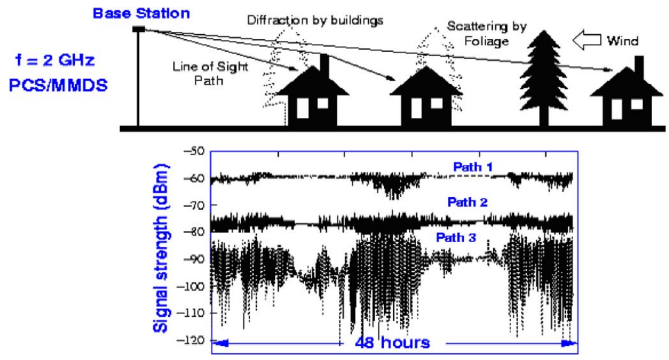

Fig. 12. Simultaneous fading observed on three fixed links in Naperville over a 48-h period.

during which fading on links to three Naperville locations were simultaneously observed (a data subset of Experiment 4).

The observation by us and others, e.g., [6]–[9], that higher wind speeds lead to lower K-factors is consistent with the picture of leaves, branches, and other objects moving in the wind and causing time variations in the sum of received rays. In our results, the correlation between wind speed at the base and the decibel K-factor was found to be -0.47; that between wind speed at the terminal and the decibel K-factor was found to be -0.56. These negative correlations are in line with our intuitive expectations.

Fig. 10 shows a scatter plot of K and wind speed, where the inverse correlation is in evidence. Each point is for a 15-min segment, and there were 96 such segments at 60 frequencies for each of the six terminal locations. For this data set, Fig. 11 shows the manner in which the mean of the K-factor (in decibels) decays with wind speed, calculated in the following wind speed intervals (in kilometers per hour): 0 (no discernible wind), (0, 2], (2, 4], (4, 8], and (8, 16]. The midpoint values of these intervals were chosen as the wind speed points on the abscissa. The steady decrease in the number of data points that we see at higher wind speeds makes it difficult to reliably estimate the standard deviation of K as a function of wind speed. Instead, we simply note that the standard deviations observed for no discernible wind is approximately 5.5 dB and that the global value over all other speeds is approximately 5.2 dB. The seemingly larger spread at zero wind speed (Fig. 10) is a result of the very large number of data points, i.e., as the number of points increases, and so does the likelihood of seeing the more extreme low-probability values.

Fig. 12 shows the signal fading experienced over a 48-h period on three different non-line-of-sight paths, from a 25-m-high base station in Naperville, IL, to three residences located within a 45° sector at distances of 600, 1000, and 1200 m. The first two paths are each obstructed by trees and structures located a few hundred meters away from the remote terminal; the latter path is obstructed by a large stand of trees that is located a few tens of meters from the remote terminal. The simultaneous onset of distinct fading events on the three links is clearly visible, but the depth of fading increases as the path becomes increasingly harsh. The high correlation between fading events on different links within the same cell has implications for radio resource management in fixed wireless systems.

We do not offer the partial results given here as a model for the dependence of K upon wind speed. We merely use them to illustrate an important physical relationship. For a meaningful model development, considerably more experimental data would be required.

V. Conclusion

We have theorized and demonstrated that narrow-band channels in fixed wireless systems can be well modeled by Ricean fading, and we have shown a simple accurate way to compute Ricean K-factors from time records of path gain magnitude. The K-factor is a key indicator of the severity of fading; therefore, modeling its statistics over fixed wireless environments is essential to the study of systems using either narrow-band or multicarrier radio techniques.

To this end, we have described the collection and reduction of a large body of data at 1.9 GHz for suburban paths in New Jersey, Illinois, and Washington. Whereas other studies have focused on locations and scenarios in which moving vehicles and pedestrians have a significant effect on fixed wireless links, we have focused on quiet residential areas where windblown trees and foliage appear to have the most significant impact. We have developed a statistical model that presents K as lognormal over time, frequency, and user location in such environments, with the median being a simple function of season, antenna height, antenna beamwidth, and distance. Moreover, we have separated the variability about the median into two parts: one due to time and frequency variations per location and one due to changes among locations. We have also demonstrated the consistency of key results across different experiments. Finally, we have produced results on the relationship of the K-factor to wind conditions. The results will be useful to those engaged in the design of fixed wireless systems and/or the modeling of fixed wireless channels.

Acknowledgment

We are indebted to numerous past and present AT&T colleagues and contractors for collecting and processing the large quantities of path loss data used in this study. They are D. J. Barnickel, M. K. Dennison, B. J. Guarino, P. B. Guerlain, D. Jacobs, S. C. Kim, R. S. Roman, A. J. Rustako, Jr., S. K. Wang, J. Lee, L. Roberts and M. Stephano.

References

[1] D. Greenwood and L. Hanzo, "Characterization of mobile radio channels," in *Mobile Radio Communications*, R. Steele, Ed. London, U.K.: Pentech, 1992, pp. 163–185.

[2] M. Schwartz, W. R. Bennett, and S. Stein, *Communication Systems and Techniques*. New York: McGraw-Hill, 1966, sec. 9.2.

[3] J. D. Parsons, *The Mobile Radio Propagation Channel*. Hoboken, NJ: Wiley, 1992, pp. 134–136.

[4] W. C. Jakes, Jr., Ed., *Microwave Mobile Communications*. New York: Wiley, 1974.

[5] M. J. Gans, N. Amitay, Y. S. Yeh, T. C. Damen, R. A. Valenzuela, C. Cheon, and J. Lee, "Propagation measurements for fixed wireless loops (FWL) in a suburban region with foliage and terrain blockages," *IEEE Trans. Wireless Commun.*, vol. 1, no. 2, pp. 302–310, Apr. 2002.

[6] E. R. Pelet, J. E. Salt, and G. Wells, "Effect of wind on foliage obstructed line-of-sight channel at 2.5 GHz," *IEEE Trans. Broadcast.*, vol. 50, no. 3, pp. 224–232, Sep. 2004.

[7] D. Crosby, V. S. Abhayawardhana, I. J. Wassell, M. G. Brown, and M. P. Sellars, "Time variability of the foliated fixed wireless access channel at 3.5 GHz," in *Proc. IEEE VTC*, May 30–Jun. 1, 2005, pp. 106–110.

[8] M. H. Hashim and S. Stavrou, "Measurements and modeling of wind influence on radiowave propagation through vegetation," *IEEE Trans. Wireless Commun.*, vol. 5, no. 5, pp. 1055–1064, May 2006.

[9] H. Suzuki, C. D. Wilson, and K. Ziri-Castro, "Time variation characteristics of wireless broadband channel in urban area," in *Proc. 1st Eur. Conf. Antennas Propag.*, Nice, France, Nov. 2006.

[10] L. Ahumada, R. Feick, and R. A. Valenzuela, "Characterization of temporal fading in urban fixed wireless links," *IEEE Commun. Lett.*, vol. 10, no. 4, pp. 242–244, Apr. 2006.

[11] R. P. Torres, B. Cobo, D. Mavares, F. Medina, S. Loredo, and M. Engels, "Measurement and statistical analysis of the temporal variations of a fixed wireless link at 3.5 GHz," *Wireless Pers. Commun.*, vol. 37, no. 1/2, pp. 41–59, Apr. 2006.

[12] R. Feick, R. A. Valenzuela, and L. Ahumada, "Experiment results on the level crossing rate and average fade duration for urban fixed wireless channels," *IEEE Trans. Commun.*, vol. 9, no. 1, pp. 175–179, Jan. 2007.

[13] L. J. Greenstein, S. S. Ghassemzadeh, V. Erceg, and D. G. Michelson, "Ricean K-factors in narrowband fixed wireless channels," in *Proc. WPMC*, Amsterdam, The Netherlands, 1999.

[14] V. Erceg, "Channel models for fixed wireless applications," *IEEE 802.16 Broadband Wireless Access Working Group, IEEE 802.16a-03/01*, Jun. 27, 2003.

[15] L. J. Greenstein, D. G. Michelson, and V. Erceg, "Moment-method estimation of the Ricean K-factor," *IEEE Commun. Lett.*, vol. 3, no. 6, pp. 175–176, Jun. 1999.

[16] C. Tepedelenlioglu, A. Abdi, and G. B. Giannakis, "The Ricean K factor: Estimation and performance analysis," *IEEE Trans. Wireless Commun.*, vol. 2, no. 4, pp. 799–810, Jul. 2003.

[17] Y. Chen and N. C. Beaulieu, "Maximum likelihood estimation of the K factor in Ricean fading channels," *IEEE Commun. Lett.*, vol. 9, no. 12, pp. 1040–1042, Dec. 2005.

[18] V. Erceg, L. J. Greenstein, S. Y. Tjandra, S. R. Parkoff, A. Gupta, B. Kulic, A. A. Julius, and R. Bianchi, "An empirically based path loss model for wireless channels in suburban environments," *IEEE J. Sel. Areas Commun.*, vol. 17, no. 7, pp. 1205–1211, Jul. 1999.

[19] V. Erceg, D. G. Michelson, S. S. Ghassemzadeh, L. J. Greenstein, A. J. Rustako, Jr., P. B. Guerlain, M. K. Dennison, R. S. Roman, D. J. Barnickel, S. C. Wang, and R. R. Miller, "A model for the multipath delay profile of fixed wireless channels," *IEEE J. Sel. Areas Commun.*, vol. 17, no. 3, pp. 399–410, Mar. 1999.

[20] S. R. Hanna and J. C. Chang, "Representativeness of wind measurements on a mesoscale grid with station separations of 312 m to 10 km," *Boundary-Layer Meteorol.*, vol. 60, no. 4, pp. 309–324, Sep. 1992.

[21] M. F. Ibrahim and J. D. Parsons, "Signal strength prediction in built-up areas. Part l: Median signal strength," *Proc. Inst. Elect. Eng.—F*, vol. 130, no. 5, pp. 377–384, Aug. 1983.

Larry J. Greenstein (S'59–M'67–SM'80–F'87–LF'02) received the B.S., M.S., and Ph.D. degrees in electrical engineering from the Illinois Institute of Technology, Chicago, in 1958, 1961, and 1967, respectively.

From 1958 to 1970, he was with IIT Research Institute, Chicago, working on radio frequency interference and anticlutter airborne radar. He joined Bell Laboratories, Holmdel, NJ, in 1970. He was with AT&T for 32 years, conducting research on digital satellites, point-to-point digital radio, optical transmission techniques, and wireless communications. For 21 years during that period (1979–2000), he led a research department renowned for its contributions in these fields. He is currently a Research Scientist with the Wireless Information Network Laboratory (WINLAB), Rutgers University, North Brunswick, NJ, working in the areas of ultrawideband, sensor networks, multiple-input–multiple-output-based systems, broadband power line systems, and radio channel modeling. He has been a Guest Editor, Senior Editor, and Editorial Board Member for numerous publications.

Dr. Greenstein is an AT&T Fellow. He is a recipient of the IEEE Communications Society's Edwin Howard Armstrong Award and a corecipient of four best paper awards. He is currently the Director of Journals for the IEEE Communications Society.

Saeed S. Ghassemzadeh (S'88–M'91–SM'02) received the B.S., M.S., and Ph.D. degrees in electrical engineering from the City University of New York, New York, in 1989, 1991, and 1994, respectively.

From 1989 to 1992, he was with SCS Mobilecom, which is a wireless technology development company, where he conducted research in the areas of wireless channel modeling. In 1992, while working toward the Ph.D. degree, he joined InterDigital, where he worked as a Principal Research Engineer, conducting research in the areas of fixed/mobile wireless channels, and was involved in system integration and testing of B-code-division multiple access (CDMA) technology. At the same time, he was also an Adjunct Lecturer with the City University of New York. In 1995, he joined AT&T Wireless Communication Center of Excellence, AT&T Bell Laboratories, where he was involved in the design and development of the fixed wireless base station. He also conducted research in areas of CDMA technologies, propagation channel measurement and modeling, satellite communications, wireless local area networks, and coding in wireless systems. He is currently Principal Member of Technical Staff with the Communication Technology Research Department at AT&T Labs-Research, Florham Park, NJ. His current research interest includes wireless propagation measurement and modeling, cognitive radio, wireless local area networks, and terahertz communications.

Dr. Ghassemzadeh is a member of the IEEE Communication Society and IEEE Vehicular Technology Society. He is currently an Associate Editor for the IEEE TRANSACTIONS ON WIRELESS COMMUNICATIONS and the *Journal of Communications and Networks*.

Vinko Erceg (M'92–SM'98–F'07) received the B.Sc. degree in electrical engineering and the Ph.D. degree in electrical engineering from the City University of New York, in 1988 and 1992, respectively.

From 1990 to 1992, he was a Lecturer with the Department of Electrical Engineering, City College of the City University of New York. Concurrently, he was a Research Scientist with SCS Mobilecom, Port Washington, NY, working on spread-spectrum systems for mobile communications. In 1992, he joined AT&T Bell Laboratories. In 1996, he joined AT&T Labs—Research as a Principal Member of Technical Staff with the Wireless Communications Research Department, where he worked on signal propagation and other projects related to the systems engineering and performance analysis of personal and mobile communication systems. From 2000 to 2002, he was with Iospan Wireless Inc., San Jose, CA, as the Director of the Communication Systems Division, working on system, propagation, deployment, and performance issues of a multiple-input–multiple-output orthogonal frequency division multiplexing communication system. He is currently a Senior Manager with the Broadcom Corporation, San Diego, CA.

David G. Michelson (S'80–M'89–SM'99) received the B.A.Sc., M.A.Sc., and Ph.D. degrees in electrical engineering from the University of British Columbia (UBC), Vancouver, BC, Canada.

From 1996 to 2001, he served as a member of a joint team from AT&T Wireless Services, Redmond, WA, and AT&T Labs—Research, Red Bank, NJ, where he was concerned with the development of propagation and channel models for next-generation and fixed wireless systems. The results of this work formed the basis for the propagation and channel models later adopted by the IEEE 802.16 Working Group on Broadband Fixed Wireless Access Standards. From 2001 to 2002, he helped to oversee the deployment of one of the world's largest campus wireless local area networks at UBC while also serving as an Adjunct Professor with the Department of Electrical and Computer Engineering. Since 2003, he has led the Radio Science Laboratory, Department of Electrical and Computer Engineering, UBC, where his current research interests include propagation and channel modeling for fixed wireless, ultra wideband, and satellite communications.

Prof. Michelson is a registered professional engineer. He serves as the Chair of the IEEE Vehicular Technology Society Technical Committee on Propagation and Channel Modeling and as an Associate Editor for Mobile Channels for *IEEE Vehicular Technology Magazine*. In 2002, he served as a Guest Editor for a pair of Special Issues of the IEEE JOURNAL ON SELECTED AREAS IN COMMUNICATIONS concerning propagation and channel modeling. From 2001 to 2007, he served as an Associate Editor for the IEEE TRANSACTIONS ON VEHICULAR TECHNOLOGY. From 1999 to 2007, he was the Chair of the IEEE Vancouver Section's Joint Communications Chapter. Under his leadership, the chapter received Outstanding Achievement Awards from the IEEE Communications Society in 2002 and 2005 and the Chapter of the Year Award from IEEE Vehicular Technology Society in 2006. He received the E. F. Glass Award from IEEE Canada in 2009.

Ricean K-Factors in Narrow-Band Fixed Wireless Channels: Theory, Experiments, and Statistical Models

Larry J. Greenstein, *Life Fellow, IEEE*, Saeed S. Ghassemzadeh, *Senior Member, IEEE*, Vinko Erceg, *Fellow, IEEE*, and David G. Michelson, *Senior Member, IEEE*

***Abstract*—Fixed wireless channels in suburban macrocells are subject to fading due to scattering by moving objects such as windblown trees and foliage in the environment. When, as is often the case, the fading follows a Ricean distribution, the first-order statistics of fading are completely described by the corresponding average path gain and Ricean K-factor. Because such fading has important implications for the design of both narrow-band and wideband multipoint communication systems that are deployed in such environments, it must be well characterized. We conducted a set of 1.9-GHz experiments in suburban macrocell environments to generate a collective database from which we could construct a simple model for the probability distribution of K as experienced by fixed wireless users. Specifically, we find K to be lognormal, with the median being a simple function of season, antenna height, antenna beamwidth, and distance and with a standard deviation of 8 dB. We also present plausible physical arguments to explain these observations, elaborate on the variability of K with time, frequency, and location, and show the strong influence of wind conditions on K.**

***Index Terms*—Fading, fixed wireless channels, K-factors, multipoint communication, Ricean distribution.**

I. Introduction

During the past decade, both common carriers and utilities have begun to deploy fixed wireless multipoint communication systems in suburban environments. For common carriers, wideband multipoint communication systems provide a method for delivering broadband voice and data to residences with greater flexibility than wired services. For utilities, narrow-band multipoint communication systems provide a convenient and independent method for controlling or monitoring the infrastructure, including utility meters located on customer premises. In the past, most narrow-band fixed wireless links were deployed in frequency bands below 900 MHz. In response to increasing demand, both the Federal Communication Commission and Industry Canada have recently allocated several new bands between 1.4 and 2.3 GHz to such applications. Because fading on fixed wireless links has important implications for the design of both narrow-band and wideband multipoint communication systems, it must be well characterized. Narrow-band fading models apply to both narrow-band signals and individual carriers or pilot tones in orthogonal frequency-division multiplexing systems such as those based upon the IEEE 802.16 standard. Ideally, such models will capture not just the statistics of fading but their dependence upon the type and density of scatterers in the environment as well.

The complex path gain of any radio channel can quite generally be represented as having a fixed component plus a fluctuating (or scatter) component. The former might be due to a line-of-sight path between the transmitter and the receiver; the latter is usually due to echoes from multiple local scatterers, which causes variations in space and frequency of the summed multipath rays. The spatial variation is translated into a time variation when either end of the link is in motion. In the case of fixed wireless channels, time variation is a result of scatterers in motion.

If the scatter component has a complex Gaussian distribution, as it does in the central limit (many echoes of comparable strength), the time-varying magnitude of the complex gain will have a Ricean distribution. The key parameter of this distribution is the *Ricean K-Factor* (or just K), which is the power ratio of the fixed and scatter components [1]–[3]. It is a measure of the severity of fading. The case $K = 0$ (no fixed component) corresponds to the most severe fading, and in this limiting case, the gain magnitude is said to be Rayleigh distributed. From the earliest days, most analyses of mobile cellular systems, e.g., [4], have assumed Rayleigh fading because it is both conservative and quite prevalent.

The case of fixed wireless paths, e.g., for wireless multipoint communication systems, is different. Here, there can still be multipath echoes, and the complex sums of received waves still vary over space and frequency. However, with both ends of the link fixed, there will be—to first order—no *temporal* variations. What alters this first-order picture is the slow motion of scatterers along the path, e.g., pedestrians, vehicles, and wind-blown leaves and foliage. As a result, the path gain at any given frequency will exhibit slow temporal variations as

Manuscript received June 26, 2008; revised December 18, 2008. The review of this paper was coordinated by Dr. K. T. Wong.

L. J. Greenstein is with the Wireless Information Network Laboratory, Rutgers University, North Brunswick, NJ 08902 USA (e-mail: ljg@winlab.rutgers.edu).

S. S. Ghassemzadeh is with the Communication Technology Research Department, AT&T Labs-Research, Florham Park, NJ 07932 USA (e-mail: saeedg@research.att.com).

V. Erceg is with the Broadcom Corporation, San Diego, CA 92128 USA (e-mail: verceg@broadcom.com).

D. G. Michelson is with the Radio Science Laboratory, Department of Electrical and Computer Engineering, University of British Columbia, Vancouver, BC V6T 1Z4, Canada (e-mail: davem@ece.ubc.ca).

Color versions of one or more of the figures in this paper are available online at http://ieeexplore.ieee.org.

Digital Object Identifier 10.1109/TVT.2009.2018549

the relative phases of arriving echoes change. Because these perturbations are often slight, the condition of a dominant fixed component plus a smaller fluctuating component takes on a higher probability than that for mobile links. Furthermore, since temporal perturbations can occur on *many* scatter paths, the convergence of their sum to a complex Gaussian process is plausible. Therefore, we can expect a Ricean distribution for the gain magnitude, with a higher K-factor, in general, than that for mobile cellular channels.

During the past decade, numerous studies have aimed to reveal various aspects of the manner in which fixed wireless channels fade on non-line-of-sight paths typical of those encountered in urban and suburban environments [5]–[12]. One set of researchers has focused on determining the manner in which wind blowing through foliage affects the depth of fading on fixed links, e.g., [6]–[9], while another has focused on scenarios in which relatively little foliage is present but scattering from vehicular traffic presents a significant impairment, e.g., [10]–[12].

In this paper, we focus on the development of statistical models that capture the manner in which fading on fixed wireless channels in suburban macrocell environments depends upon the local environment, the season (leaves or no leaves), the distance between the base and the remote terminal, and the height and beamwidth of the terminal antenna. We do so using an extensive body of data collected during four distinct experiments. Our earlier findings were presented in [13] and were ultimately adopted by IEEE 802.16 [14]. Here, we fill in the essential detail concerning the measurement campaigns and present plausible physical arguments to explain our observations. Furthermore, we demonstrate that the variability of the channel about the median can be divided into a component due to variation at a fixed location and another due to variation between locations. Finally, we present what we believe are the first observations of simultaneous fading events on different links within the same suburban macrocell.

In Section II, we review a method for computing K from time records of path gain magnitude that is particularly fast and robust and therefore suited to high-volume data reductions. We show that it is also highly accurate. In Section III, we describe several experiments that were conducted at 1.9 GHz to measure path gains on fixed wireless links. The data from these experiments were used to compute K-factors for narrow-band channels. In Section IV, we show how the computed results were used to model the statistics of K as a function of various parameters. We also examine such issues as the variability of K with time, frequency, and location and the influence of wind conditions on K. Section V concludes the paper.

II. Estimation of Ricean K-Factor

A. Background

Our practical objective is to model narrow-band fading by means of a Ricean distribution over the duration of a fixed wireless connection. We assume that the duration of a connection is in the 5–15-min range, and we will compute K for finite time intervals of that order. Later, we will show how K can vary with the time segment and with frequency. We will also show that the statistical model for K is very similar for 5- and 15-min intervals.

B. Formulation

We characterize the complex path gain of the narrow-band wireless channel by a frequency-flat time-varying response

$$g(t) = V + v(t) \tag{1}$$

where V is a fixed complex value, and $v(t)$ is a complex zero-mean random time fluctuation caused by vehicular motion, wind-blown foliage, etc., with variance σ^2. This description applies to a particular frequency and time segment. Both V and σ^2 may change from one time–frequency segment to another.

We assume that the quantity actually measured is the received narrow-band power, which, suitably normalized, yields the instantaneous power gain

$$G(t) = |g(t)|^2 . \tag{2}$$

Various methods have been reported to estimate K using moments calculated from time series such as (2), e.g., [15]–[17].

We can relate K to two moments that can be estimated from the data record for $G(t)$. The first moment G_m is the average power gain; its true value (as distinct from the estimate

$$G_m = \sum_{i=1}^{N} \frac{G_i}{n} \tag{3}$$

computed from finite data) is shown in [15] to be

$$G_m = |V|^2 + \sigma^2. \tag{4}$$

The second moment G_v is the RMS fluctuation of G about G_m. The *true* value of this moment (as distinct from the estimate

$$G_v = \sqrt{\frac{1}{N}\sum_{i=1}^{N}(G_i - G_m)^2} \tag{5}$$

calculated from finite data) is shown in [15] to be

$$G_m = \sqrt{\sigma^4 + 2|V|^2\sigma^2}. \tag{6}$$

In each of (4) and (6), the left-hand side can be estimated from the data, and the right-hand side is a function of the two intermediate quantities we seek. Combining these equations, we can solve for $|V|^2$ and σ^2, yielding

$$|V|^2 = \sqrt{G_m^2 - G_v^2} \tag{7}$$

$$\sigma^2 = G_m - \sqrt{G_m^2 - G_v^2}. \tag{8}$$

Finally, K is obtained by substituting these two values into

$$K = |V|^2/\sigma^2. \tag{9}$$

Note that σ^2 as defined here is twice the RF power of the fluctuating term, which is why the customary factor of two

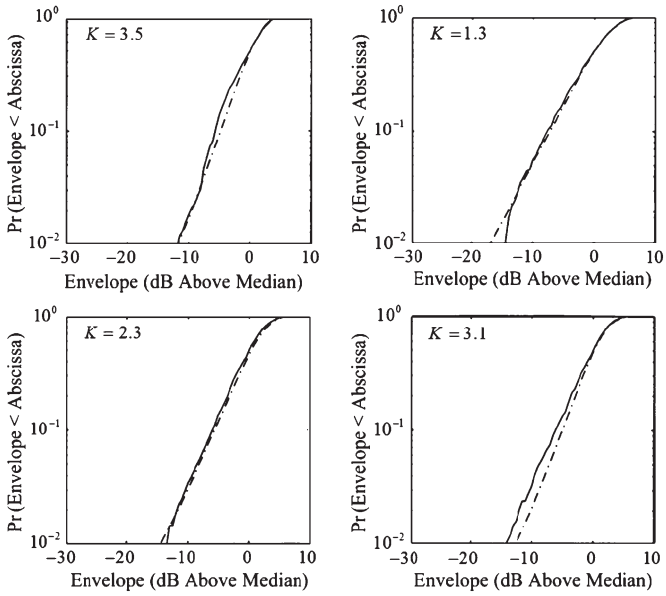

Fig. 1. Four typical envelope cdf's, comparing actual data (solid curves) with Ricean distributions (dashed curves). The latter use K-factors derived from data via the moment method.

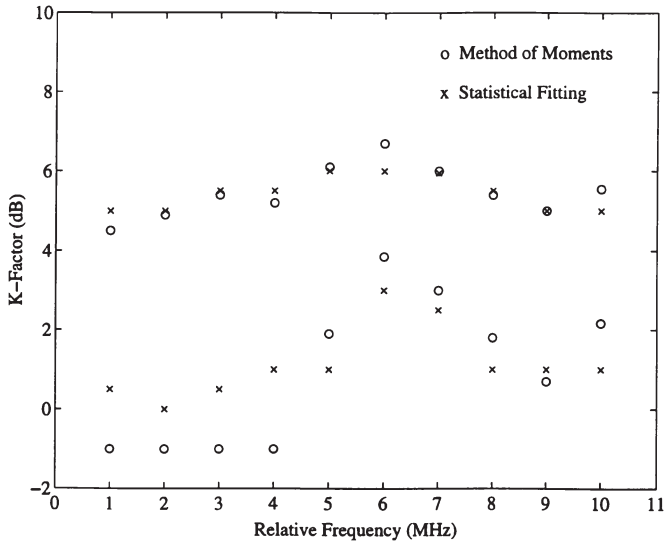

Fig. 2. Comparisons, for each of two locations, of K versus f, where K is derived via two methods: the moment method and the least-mean-square fitting of empirical and Ricean distributions. These results are typical and show that the moment method predicts K to within 2 dB (usually much less) of the results for least-mean-square fitting.

(see [3, eq. (5.60)]) is not present in (9). The K-factor and average power gain G_m jointly determine the Ricean envelope distribution.

The choice of the measurement interval is a necessary compromise between obtaining a large sample size and preserving the stationarity within the interval. Given the rate at which meteorological conditions, particularly wind conditions, usually change, we considered 15 min to be suitably small. This supposition is supported by the consistency of our results for 5- and 15-min segments.

C. Validation

For each of several fixed wireless paths located in suburban New Jersey, we collected 5-min time sequences of received power at 1.9 GHz (see Section III). For each path, we can compute a cumulative distribution function (cdf) of the measured samples. This is the empirical cdf of the received envelope. We can also estimate G_m and K, the two parameters that define a Ricean distribution, and then compute a Ricean distribution that should closely match the empirical one.

Comparisons for four typical cases are shown in Fig. 1. Each corresponds to a particular time, frequency, and transmit–receive path. In each case, the results show that, although some cases fit better than others, the Ricean distribution obtained using the estimated moments is quite close to the empirical one. Deviation from the ideal can usually be interpreted as the result of a transient fading event affecting the distribution of either the fixed or scatter component. In the absence of more detailed information, e.g., time- and/or angle-of-arrival data, it is difficult to offer further interpretation of a given result.

We also examined goodness-of-fit methods to determine K. Although they are accurate, they are also much more time intensive and, thus, not conducive to the reduction of large quantities of data [1]. Moreover, they produce results not much different from those using the moment method. Fig. 2 gives two typical comparisons, based upon data collected in suburban New Jersey, in each of which K-factors at different frequencies over a 9-MHz bandwidth are shown for both the moment method and the goodness-of-fit method. The latter consisted of matching the data-derived cdf of G to a Ricean one, with K chosen to minimize the RMS decibel difference between cdf's over the probability range from 1% to 50%.

We note that, if the calculated moment G_v exceeds the calculated moment G_m, the calculated result for $|V|^2$, from (7), will be imaginary. When this happens, it is because either 1) the underlying process is not well modeled as Ricean, or 2) the statistical noise of the finite time record produces a G_v slightly larger than G_m instead of being equal to or slightly smaller than G_m.

In our reductions, we declare K to be 0.1 if G_v exceeds G_m by less than 0.5 dB[1]; if it is larger than that, we remove the particular record from the database. In our reductions of 5-min records, such removals occurred in a small fraction of all cases (less than 2%). In our reductions of 15-min records, the fraction was even smaller.

Typical 5-min records of received decibel power are shown in Fig. 3. Such records, converted to linear power and suitably normalized, yield records of $G(t)$, as given in (2). Our examination of data like these indicate that relatively shallow fluctuations, on a time scale of 1 or 2 s, occur on most links, in addition to possibly deeper fluctuations on a time scale of tens of seconds [18].

D. Properties of the Ricean K-Factor

The complex fluctuation $v(t)$, from (1), for a given frequency is due to temporal variations in gain on one or more paths. If these variations are independent among paths, then the

[1]Over the range below 0.1, the precise value of K is immaterial. For all practical system purposes, it is zero, but we assign it a value 0.1 (-10 dB) for convenience in tabulating statistics.

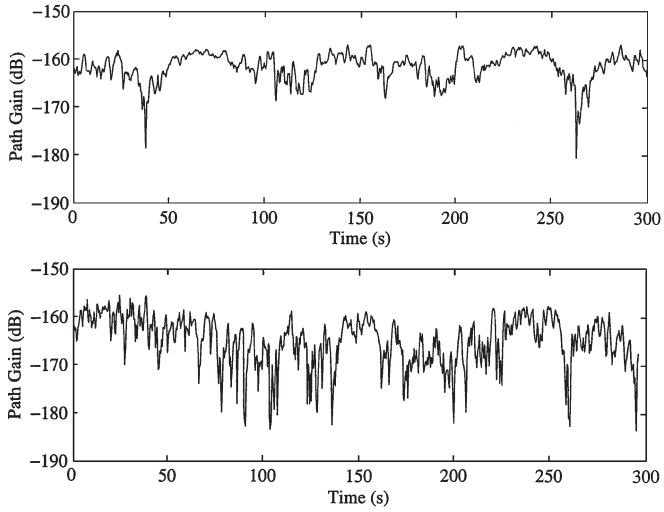

Fig. 3. Two typical examples of measured path gain at a particular frequency over 280 s. Note that fading can be quite deep and that temporal fluctuation rates are on a scale of hertz or lower.

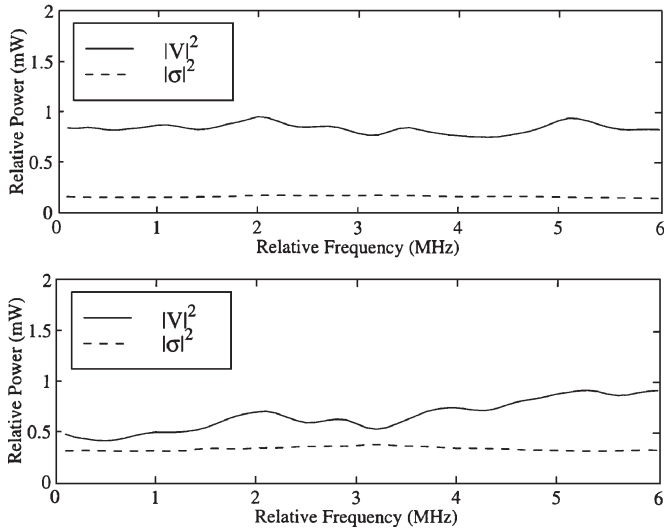

Fig. 4. Two typical examples of the fixed and mean-square "scatter" components of path gain, as functions of frequency. Note that σ^2 is fairly flat with frequency, so that the frequency variation of $K = |V|^2/\sigma^2$ follows that of $|V|^2$.

mean-square value of $v(t)$ will be flat with frequency. [To see this, write $v(t)$ as the response at a given frequency to a sum of delayed echoes, where the echoes have time-varying independent gains of zero mean. Next, derive the ensemble mean of $|v(t)|^2$, and note that it is independent of the given frequency.] This result is observed in the sample plots, in Fig. 4, of $|V|^2$ and σ^2 versus frequency. These plots are typical of what we observe on most links, i.e., σ^2 exhibits a relative flatness with frequency, with the small perturbations being attributable to statistical effects. Since K is the ratio of $|V|^2$ to σ^2, we conclude that its variation with frequency is essentially proportional to that of the fixed gain component. This, in turn, depends on the complex amplitude versus delay of the significant echoes, which varies from one transmit–receive path to another [19].

Other properties of the Ricean K-factor can be anticipated by similar reasoning.

1) At a given distance, we might suppose that the strength of the scatter component, which is the result of rays coming from a multiplicity of directions, will vary far less than the strength of the fixed component, which is dominated by rays coming from the direction of the base station and which will be strongly affected by local shadowing along that direction. Thus, we expect K to exhibit lognormal statistics across locations, with a standard deviation comparable to that associated with shadow fading.
2) By definition, remote terminals in macrocell environments generally lie in the shadow region of the obstacles that block its line of sight to the base station. As the height of the terminal antenna increases, the diffraction angle will decrease, and the strength of the fixed component will increase. Again, we might suppose that the scatter component, which is the result of reflection and scattering from a multiplicity of directions, will vary far less with the terminal height than the fixed component. Thus, we expect K to increase with the terminal height.
3) Because the scattered component will come from all other directions, increasingly less of the scatter signal will be received as the beamwidth of the receiving antenna decreases. Thus, we expect K to increase as the antenna beamwidth decreases.
4) Previous work has shown that the average wind velocity above treetop level does not vary much over distances of several kilometers [20]. Thus, we expect that fading events associated with windblown foliage should be fairly well correlated between links within a typical cell.

In the next section, we describe the experiments that we conducted to investigate the validity of these and other conjectures.

III. Measurement Program

The database used in our modeling comes from four distinct experiments conducted in suburban areas, as summarized in Table I. Each of the four experiments has its own purposes, strengths, and limitations but had, as one of its objectives, the determination of K-factors on fixed wireless paths. Collectively, this set has provided an extensive body of data from which Ricean K-factors can be computed and modeled. We describe the four experiments in this section and report the K-factors reduced from them in the next section. It should be noted that fading on the uplink and downlink are reciprocal for the same path and frequency and that all the measurements reported here were for the downlink only. Furthermore, all measurements were made using an equipment van parked on the street, with the terminal antenna pointed to receive the maximum downlink signal. All of our data were collected in quiet residential neighborhoods with minimum residential and pedestrian traffic.

We characterized each neighborhood according to the general nature of both the terrain and the trees and foliage but did not attempt to characterize vegetation density or building-to-lot area ratios along individual paths. Whereas such an approach was used in [21] to assist in the prediction of mean path loss in urban environments, our measurement database, large as it is, is insufficient to take full advantage of such detail.

TABLE I
SUMMARY OF THE FOUR EXPERIMENTS

Exp. No.	Measurement parameters	Measurement Duration	Terminal Antenna	Geography, Seasons	Uses for Reduced Data
1	9 MHz (90 frequencies) Base Antenna: Single-pol Panel h=15 and 30m	5-minute samples at each downlink location.	Single-pol; b = 17°, 30°, 65°; h = 3 m, 10 m	Three transmit sites in NJ. Tens of downlink locations for each site. Summer and Winter.	Devise first-order model for pdf of K at any time, frequency and location in NJ suburban environments.
2	CW (one frequency) Base Antenna: Single-pol Omni-directional h=25m	5-minute samples at each downlink location.	Single-pol; b = 45° and omni antenna; h = 3 m	One transmit site in WA, two in IL. Tens of downlink locations for each site. Summer only	Reinforce first-order model. Examine regional differences. Show effects of omni vs. directional antennas.
3	6 MHz (60 frequencies) Base Antenna: Single-pol Panel h=15 and 30m	Long runs (12 – 24 hrs) at each downlink location.	Dual-pol; b = 32°; h = 3 m	Two transmit sites in NJ. Seven and nine downlink sites. Summer only.	Reinforce first-order model. Examine variations with time and frequency.
4	CW (one frequency) Base Antenna: Single-pol Omni-directional h=25m	Long runs (2 – 12 hrs) at each downlink location.	Dual-pol; b = 32°; h = 3 m	Two transmit sites in IL. 14 and 21 downlink locations. Summer only.	Reinforce first-order model. Examine regional differences. Examine variations with time.

A. *Experiment 1: Short-Term Measurements in New Jersey*

Downlink measurements were made for three transmit sites in northern and central New Jersey. For each site, data were collected at 33 or more downlink locations during summer (trees in full bloom), and repeat measurements were made at half or more of these locations during winter (trees bare). Distances ranged (more or less uniformly) from 0.5 to 9 km. This was the major experiment in our study, and so, we summarize a number of its features in Table II.

The transmit sites were located in the residential communities of Holmdel, Whippany, and Clark. Each site overlooked a terrain consisting of rolling hills with moderate to heavy tree densities and dwellings of one or two stories. Furthermore, each site used a panel-type transmitting antenna with elevation and azimuth beamwidths of 16° and 65°, respectively. The antenna was fed by a 10-MHz swept frequency generator centered at 1985 MHz.

For each downlink location (i.e., receive terminal site) for each of two antennas at each of two heights (3 and 10 m), the data record consists of 700 "snapshots" of received power versus frequency. The receiver was a swept frequency spectrum analyzer equipped with a low noise amplifier to increase its sensitivity; its sweep was synchronized to that of the transmitter using the 1-pulse-per-second signal from a GPS receiver. The unit was operated in sample detection mode to enhance its ability to characterize the first-order statistics of random signals. A local controller handled the configuration, operation, and data acquisition. The "snapshots" for each antenna/height combination are spaced by 0.4 s, for a total time span of nearly 5 min, and each consists of 90 samples, spaced by 100 kHz, for a frequency span of 9 MHz. In the data processing, the power samples, which were recorded in decibels of the measured power referenced to 1 mW (dBm), were calibrated and converted to linear path gain.

TABLE II
FEATURES OF EXPERIMENT 1

Transmit Site (Location, Antenna Height)	Terrain	Number of Downlink Locations	Terminal Antenna (Azimuth Beamwidth, Height)
Holmdel, 15 m	Rolling hills, moderate-to-heavy tree density with some close-in tree blockage, 1 – 2 story dwellings within the transmitting sector.	44 Summer, 44 Winter	Dish; b = 17° Panel; b = 65° h = 3 m and 10 m
Clark, 15 m	Rolling hills, moderate-to-heavy tree density, 1 – 2 story dwellings and some commercial buildings within the transmitting sector.	33 Summer, 14 Winter	Two panel antennas, spaced by 1.8 m; b = 30° h = 3 m and 10 m
Whippany, 30 m	Rolling hills, moderate-to-heavy tree density, 1 – 2 story dwellings within the transmitting sector.	37, Summer, 20 Winter	Two panel antennas, spaced by 1.8 m; b = 30° h = 3 m and 10 m

B. Experiment 2: Short-Term Measurements in Illinois and Washington

During the spring and summer, measurements were made in the vicinity of a transmit site in Washington (Redmond, near Seattle) and from two transmit sites in Illinois (Bellwood and Naperville, near Chicago). The number of downlink locations was more than 100 for each transmit site at distances ranging from 0.4 to 2.2 km.

All three transmit sites were in suburban/residential environments. The Redmond site overlooked a hilly terrain with heavy tree cover. The Bellwood and Naperville sites overlooked an extremely flat terrain with high and low tree densities, respectively. The measurement data were collected using a continuous-wave (CW) transmitter and multichannel narrowband measurement receiver manufactured by Grayson Electronics. The amplitude resolution was 1 dB, which was deemed to be adequate for the purpose of determining K.

Two antennas were used at each downlink location: one directional and one omnidirectional. They were used to simultaneously make measurements and were both mounted at a height of 3 m. No measurements were made in winter. Each measurement consisted of recording the received signal power at a rate of 400 samples/s for 5 min.

C. Experiment 3: Long-Term Measurements in New Jersey

Long-term measurements (record lengths of up to 24 h) were made from two transmit sites in northern New Jersey: one in Iselin and one in Whippany. The Whippany site was the same as the one used in Experiment 1. The Iselin site used a similar transmit antenna, at a height of 15 m, and overlooked a residential area similar to that in Whippany. The total number of downlink locations processed for these two sites was 16, with distances ranging from 0.5 to 3.1 km.

The measurement approach was similar to that for Experiment 1: The received power was recorded at 100 frequencies over 10 MHz centered on 1985 MHz. The three main differences were 1) the reception was on the two branches of a slant-45° dual-polarized antenna with an azimuth beamwidth of 32°, 2) data were recorded for continuous intervals ranging from 11 to 24 h, and 3) the wind speed was continuously measured and recorded at both ends of the path.

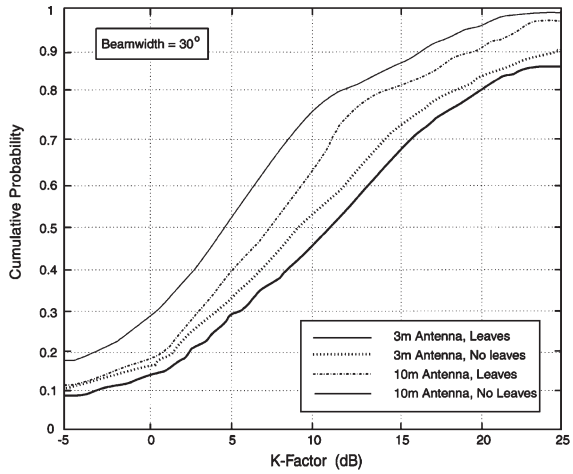

Fig. 5. CDFs of the K-factor for an antenna beamwidth of 30°. These results are for New Jersey locations measured in Experiment 1.

In the data reductions, only the central 6 MHz of data were processed (60 frequencies), and the long time records were parsed into 15-min segments. Thus, a 24-h recording produced a 96 × 60 matrix of time–frequency segments, and K was computed for each one. This permitted us to obtain K for time segments longer than the original 5-min samples as well as to examine slow variations in K over the course of a day. The decision to limit the number of frequencies processed was a business decision that does not materially affect the results. Indeed, the fact that single-carrier and multicarrier results with different parameters yield consistent results gives us greater confidence in the generality of our findings.

D. Experiment 4: Long-Term Measurements in Illinois

Long-term measurements were made from two transmit sites in Illinois, i.e., the same Bellwood and Naperville sites used in

TABLE III
MEDIAN K-FACTORS FOR EXPERIMENT 1*

Antenna Beamwidth, b	Summer (Leaves)		Winter (No Leaves)	
	h = 3 m	h = 10 m	h = 3 m	h = 10 m
17°	6.0 dB	8.0 dB	10.0 dB	12.5 dB
30°	4.5 dB	7.5 dB	9.0 dB	11.0 dB
65°	2.5 dB	5.0 dB	6.0 dB	8.5 dB

* All values have been rounded to the nearest 0.5 dB.

Experiment 2. For Bellwood, there were 14 downlink locations, at distances ranging from 0.35 to 1.4 km; for Naperville, there were 21 downlink sites, at distances ranging from 0.6 to 2.1 km.

The measurement approach was similar to that of Experiment 2, with differences similar to those between Experiments 1 and 3: 1) the use of dual-polarized slant-45° antennas with 32° beamwidths; 2) the long-term data records, with measurements ranging from 2 to 12 h; and 3) the measurement and recording of wind speed.

IV. RESULTS

A. First-Order Statistical Model for K

General: By a "first-order statistical model," we mean one that gives the probability distribution of K, given a set of path and system parameters, e.g., distance, season, terminal antenna height, and terminal antenna beamwidth, based upon measurements collected over time, frequency (in the case of multicarrier signals), and location. A "second-order statistical model" would, in addition, sort out the individual variations with time, frequency, and location. We provide some results on that aspect in Section IV-C.

The model we present here is entirely based on the database for Experiment 1, which is the richest in terms of parameter variation. However, we will expand this model and confirm its validity by using results from the other three experiments.

Database: Each short-term measurement in New Jersey initially produced 750 "snapshots," spaced by 0.4 s, of received power versus frequency at 100 frequencies spaced by 100 kHz. For convenience in the data reductions, however, each record was trimmed to 700 "snapshots" (280-s time span) and 90 frequencies (9-MHz frequency span). We thus computed 90 K-factors, each using recorded power versus time over 4.67 min. In only 1% of all cases did the method in Section II fail to produce a real solution for K.

K-Factor Medians: As noted in Table I, the database encompasses two seasons [summer (leaves) and winter (no leaves)], two antenna heights (3 and 10 m), and three antenna beamwidths (17°, 30°, and 65°), for a total of 12 combinations. For each parameter set (season, height, and beamwidth), we computed K over a large population of frequencies and locations and then computed a cdf. One such result is shown in Fig. 5, which shows four cases (2 seasons $\times$ 2 heights) for a given beamwidth. To compress the information in curves like this, we extracted the median K for all the cdf's and analyzed the 12 values. These values are summarized in Table III, rounded to the nearest 0.5 dB.

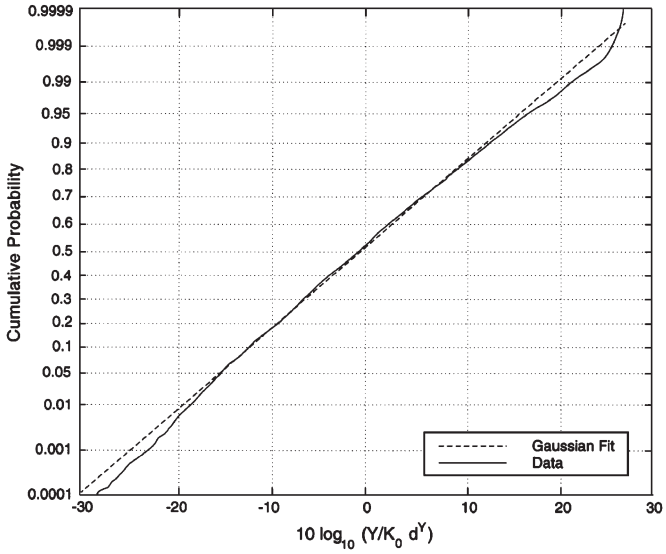

Fig. 6. CDF of the K-factor variation about the distance regression line for the data of Experiment 1. The closeness to a straight line on this scale implies a near-lognormal distribution. The slope implies a standard deviation of 8 dB.

Methodology: First, we examine the influence of season (leaves versus no leaves). For the six combinations of two antenna heights and three antenna beamwidths, we see a consistent increase in median K from summer to winter, ranging from 3.5 to 4.5 dB with an average close to 4.0 dB (or 2.5 in linear units). We attribute the increase to the reduction in gain variations when there are no windblown leaves.

Second, we examine the influence of antenna height h. For the two seasons and three beamwidths, we see a consistent increase from 3 to 10 m, ranging from 2.0 to 3.0 dB with an average of 2.4 dB. If we assume a power-law relationship, i.e., $K \propto h^{\alpha}$, then $\alpha = 0.46$. This modest increase with h is consistent with intuition: we expect there to be a gradual increase in line-of-sight power (which is generally fixed in time) as the terminal antenna height increases. In hindsight, it would have been preferable to collect data at three heights rather than just two. On the other hand, such trends, particularly over a limited range of values as in this case, are almost always approximately linear on a log–log plot, indicating a power-law relationship. It is unlikely that the true decibel values for

TABLE IV
SUMMARY OF RESULTS FOR EXPERIMENT 2

Antenna	Site	Distance Exponent, γ	1 km Intercept, K_1 (dB)	σ(dB)
	Naperville, IL	-0.35	5.6	5.3
Omni-directional	Bellwood, IL	-0.20	1.9	4.1
	Redmond, WA	-0.42	5.5	5.6
	Naperville, IL	-0.52	12.3	5.2
Directional	Bellwood, IL	-0.30	8.0	3.4
	Redmond, WA	-0.12	11.6	6.4

heights in between would seriously be different from what the power-law relationship predicts. Because the behavior of K with height will change as the terminal antenna rises out of the local clutter, care should be taken not to extrapolate beyond the height of the clutter.

Third, we examine the influence of antenna beamwidth b. In the Holmdel measurements, beamwidths of 17° and 65° were used in simultaneous measurements. The difference in median K between these two beamwidths ranges from 3.0 to 4.0 dB, with an average of about 3.6 dB. If we assume a power-law relationship, i.e., $K \propto b^{\beta}$, then $\beta = -0.62$. When we apply this law to the medians for $b = 30°$, which were collected elsewhere (Clark and Whippany), the agreement is within 1 dB.

The result for β is particularly satisfying. If there was no angular scatter, we would expect to see $\beta = 0$ (K-factor unaffected by beamwidth), and if the scatter were uniform in strength over 360° in azimuth, we would expect to see $\beta = -1.0$ (K-factor directly proportional to antenna gain). The value $\beta = -0.62$ is consistent with an environment of significant but not totally uniform scatter.

Finally, we consider the influence of distance d. If we assume a power-law relationship, i.e., $K \propto d^{\gamma}$, then the aforementioned results lead us to the formulation

$$K \cong F_s F_h F_b K_o d^{\gamma} \ (d \text{ in kilometers}) \tag{10}$$

where the factors are defined as follows.

1) F_s is the seasonal factor

$$F_s = \begin{cases} 1.0, & \text{Summer (Leaves)} \\ 2.5; & \text{Winter (No Leaves).} \end{cases} \tag{11}$$

2) F_h is the height factor

$$F_h = (h/3)^{0.46} \ (h \text{ in meters}). \tag{12}$$

3) F_b is the beamwidth factor

$$F_b = (b/17)^{-0.62} \ (b \text{ in degrees}). \tag{13}$$

K_o and γ are constants to be optimized via regression fitting. Now, we form the data variable

$$Y = K/(F_s F_h F_b) \cong K_o d^{\gamma}. \tag{14}$$

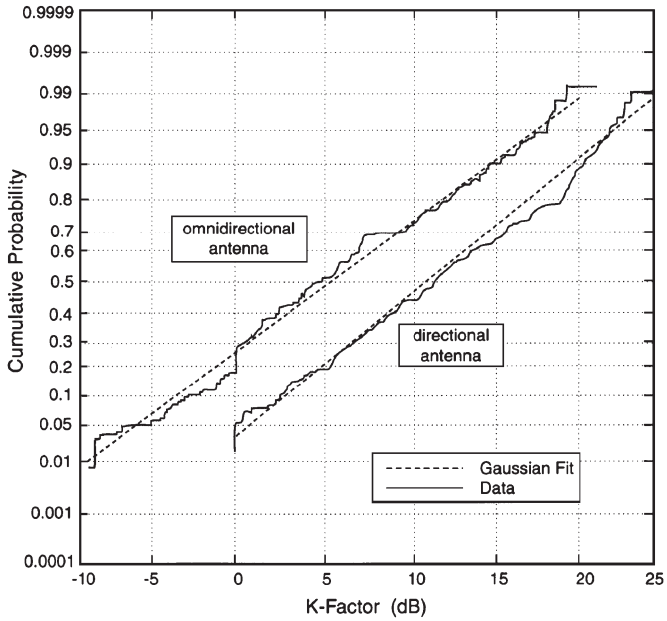

Fig. 7. CDFs of the K-factors computed for Naperville, IL, in Experiment 2. Both results show near-lognormal distributions. The standard deviation is similar for each (slightly above 6 dB), but the median for the directional antenna is roughly 6 dB higher than that for the omnidirectional antenna.

For every K computed in the database, there is an associated season, height, beamwidth, and distance, and so, a Y value can be computed and paired with d. We can then perform a regression fit between Y and d over the database.[2]

The result we get is that $K_o \cong 10.0$ dB and $\gamma \cong -0.5$ dB. The standard deviation of 10 log Y about the regression curve is just under 8.0 dB. Moreover, the distribution of 10 log Y about that curve is very nearly Gaussian, as seen in Fig. 6. The meaning is that K can be very accurately modeled as a lognormal variable, with a median value easily related to path and system parameters.

Summary of the First-Order Model: At any time, frequency, and location, the K-factor in a given season, for a given antenna

[2]We are implicitly assuming a common distance dependence for all parameter combination, which is an assumption not fully vindicated by the data. We will see that the price for this simplification is a modest increase in variability about the median.

TABLE V
SUMMARY OF RESULTS FOR EXPERIMENT 4

Distance	Site	Median K (dB)		σ (dB)	
		Branch 1	**Branch 2**	**Branch 1**	**Branch 2**
$d < 1$ km	Naperville, IL	16.7	16.6	4.6	3.5
	Bellwood, IL	14.9	14.6	3.4	3.1
$d \geq 1$ km	Naperville, IL	17.9	17.6	6.2	4.8
	Bellwood, IL	14.8	13.4	5.3	6.1

height, antenna beamwidth, and distance, can be described as follows in a suburban New Jersey type of terrain:

$$K = K_1 d^{\gamma} u \tag{15}$$

where K_1 is the 1-km intercept

$$K_1 = F_s \cdot F_h \cdot F_b \cdot K_o \tag{16}$$

$K_o \cong 10.0$ dB; $\gamma \cong -0.5$; F_s, F_h, and F_b are given by (9)–(11); and u is a lognormal variate, whose decibel value is zero mean with a standard deviation σ of 8.0 dB.

We observe that, for each of the 12 parameter sets identified earlier, the standard deviation about the decibel median for that set was about 7 dB, or a bit more. The increase of less than 1 dB in σ is mostly due to simplifications in modeling the median, including assuming a common distance dependence for all parameter sets. This small degree of added variability is a minor price for obtaining a simple and user-friendly model.

B. Consistency Checks

The reduced results from Experiment 2 are summarized in Table IV. In computing K via (1)–(9), the percentage of data removed because K was not real was 0%, 1%, and 2% for Redmond, Naperville, and Bellwood, respectively, with no difference between omnidirectional and directional antennas. We make the following observations.

1) The main difference between the terrains in Bellwood and Naperville is tree density (high in Bellwood and low in Naperville). The roughly 4-dB higher values for K_1 in Naperville (3.7 and 4.3 dB for omnidirectional and directional antennas, respectively) match the seasonal difference for New Jersey (leaves versus no leaves).
2) The higher values of K_1 for the directional antennas closely follow the beamwidth dependence given by (13), which predicts a 5.6-dB increase for the 45° beamwidth used in Illinois and a 6.7-dB increase for the 30° beamwidth used in Washington. The agreements (within 1 dB) are exceptionally good, particularly since (13) was empirically derived for beamwidths of 65° and below.
3) The values of K_1 for Bellwood and Naperville (taking proper account of the beamwidth and season) are within 0.5 dB of the values predicted by the first-order model.
4) The numerical values for γ and σ in Table IV are consistent with those for the first-order model. The distance exponent is smaller in some cases, and so is the standard deviation. However, the data volume for Experiment 2 is not large enough for these differences to be statistically significant. What the tabulations show that is significant is that σ does not change with antenna beamwidth, in agreement with the first-order model.
5) The cdf's of K in Illinois and Washington show the same lognormal character predicted by the first-order model. For example, Fig. 7 shows cdf's of K, for both antenna types, in Bellwood.

Now, moving to Experiment 3, we present a result that shows a remarkable consistency with the first-order model: Over 60 frequencies and up to 96 time segments at 16 locations, K was found to be essentially lognormal, with a median and standard deviation of 8.5 and 7.1 dB, respectively. Since these data were for distances uniformly clustered between 0.5 and 2.0 km, the median closely corresponds to the 1-km intercept of the model, i.e., K_1 in (16). For the conditions summer, $h = 3$ m, and $b = 32°$, the model predicts K_1 to be 8.3 dB. Furthermore, the 7.1-dB standard deviation is close to the 8.0-dB model value, which is slightly elevated due to modeling approximations.

Note that Experiments 1 and 3 were conducted on different paths, in different years, using two different measurement intervals (5 and 15 min) and different antenna types. Given all that, the agreement in the global statistics of K is indeed remarkable.

Somewhat less affirming is a comparison with the results from Experiment 4, summarized in Table V. On the positive side, these results repeat the increase in median K-factor at Naperville relative to Bellwood (an average of about 2.7 dB). On the other hand, the median K-factors for both sites are several decibels higher than those predicted by the model (an average increase of about 6 dB), and the standard deviations are 1–3 dB lower. A plausible explanation is the lower tree densities, for *both* sites, relative to those in New Jersey. If the wind-induced motion of trees (branches and leaves) is a significant cause of path gain variations, then we should expect to see tree density as a separate determinant of the K-factor. The comparisons here between the Illinois and New Jersey data may be a step toward establishing such a correspondence.

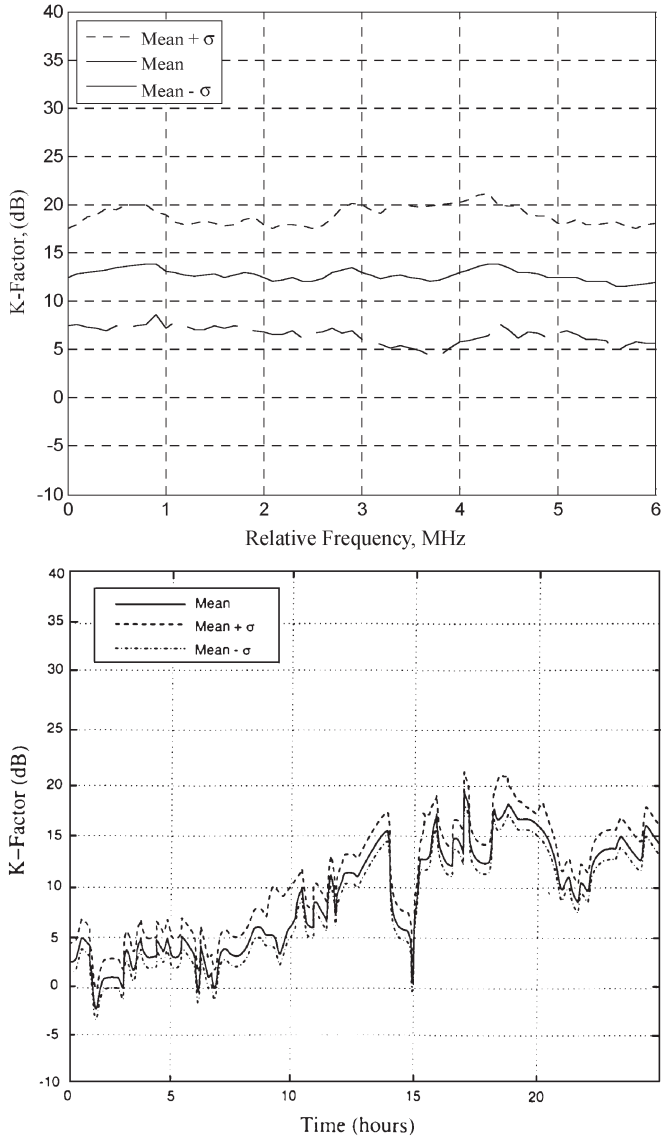

Fig. 8. Variation of K with (top) frequency and (bottom) time. The results shown are for a typical path. The standard deviation (σ) for the top graph is computed over 96 15-min intervals at each frequency; for the bottom graph, it is computed over 60 frequencies in each 15-min time interval. Note the relative constancy of the results with frequency but not time.

C. Variations With Time, Frequency, and Location

The variation of K with time at a given frequency is due to slow changes of various kinds, e.g., changes in physical objects within the environment and wind conditions. (Temperature and humidity have a significant effect on long-distance point-to-point links because they affect both the refractive index profile and the atmospheric turbulence; their possible role in impairing non-line-of-sight fixed wireless systems is an area for further study.) The variation in K with frequency at a given time is due to a multipath, which causes frequency-selective variations in the RF gain. Taken together, the time/frequency variations at a given location account for a significant part of the K-factor variability reflected in the first-order model.

However, another significant component is the variation among locations. For analysts doing system simulations, it is important to separate the two kinds of variability, as their impacts are different. We can do this separation by expressing the decibel value of u, from (15), as

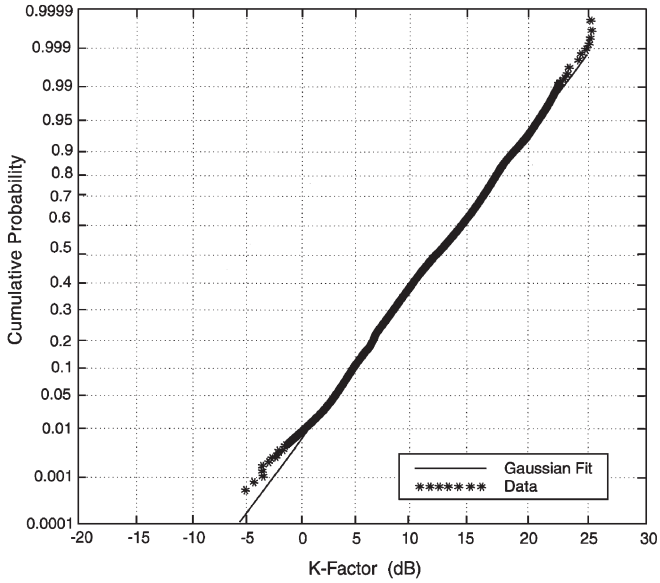

Fig. 9. CDF of K for a given location, computed over 96 15-min intervals at each of the 60 frequencies. For this typical case, the variation of K with time and frequency at a given location is seen to be essentially lognormal.

$$10 \log u \equiv U_{\mathrm{TF}} + U_{\mathrm{LOC}} \tag{17}$$

where U_{TF} and U_{LOC} are independent zero-mean Gaussian variates with standard deviations of σ_{TF} and σ_{LOC}, respectively. U_{TF} varies at a given location as a function of time of connection and frequency assignment; U_{LOC} is fixed at a given location but varies among locations over the terrain. The RMS sum of the two standard deviations is σ in the first-order model.

To make these points more concrete, Fig. 8 (top) shows the variability of the decibel K-factor for a particular New Jersey path over 6 MHz and 24 h. This plot conveys the median and standard deviation of K, computed over a 24-h period, i.e., over 96 15-min segments, as a function of frequency. Note that the variability at any given frequency can be severe, e.g., the $\pm\sigma$ region can span a range from 4 to 21 dB. Furthermore, there is roughly uniform behavior with respect to frequency, i.e., there are no "preferred" frequencies at the chosen location. This general observation applies to other locations as well.

Another version of the same data [Fig. 8 (bottom)] conveys the median and standard deviation, computed over 6 MHz, i.e., over 60 frequencies, as a function of time. Here, the spread in frequency at a given time is small. This spread depends on the delay profile of the channel and can significantly vary from one location to another, as we have observed [19]. Furthermore, there can be "good" time periods (high K) and "bad" time periods (low K), as we see in this example.

The variability of K over time and frequency was evaluated for each of the 16 downlink locations in the database of Experiment 3. First, we found that the variability is well described as lognormal, as exemplified in Fig. 9. Second, the standard deviation of K per location had an average value of 5.7 dB, with a fairly narrow spread across the 16 locations. The median of K per location had a standard deviation across locations of

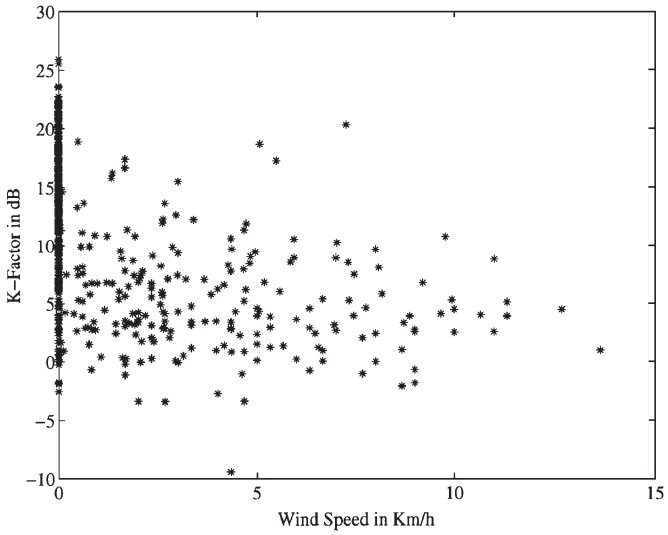

Fig. 10. Scatter plot of K-factor and wind speed for six New Jersey locations.

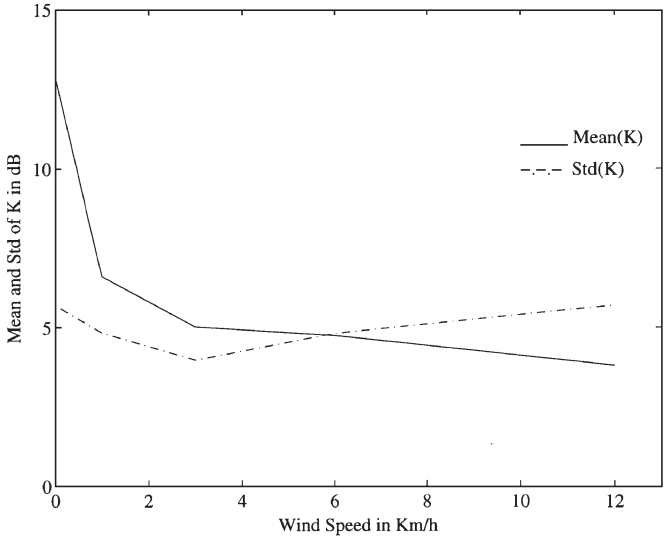

Fig. 11. Mean and standard deviation of the decibel K-factor as functions of wind speed for the six New Jersey locations. The general inverse relationship of K and wind speed is evident.

4.3 dB. The RMS sum of the two standard deviations is 7.1 dB, which we cited earlier as the global value over time, frequency, and location.

We propose that, in the lognormal model for K, 10 log u should be decomposed as in (17), with $\sigma_{\mathrm{TF}} = 5.7$ dB and $\sigma_{\mathrm{LOC}} = 5.6$ dB, the latter being larger than 4.3 dB to reflect our imperfect modeling of the median K (see Section IV-A). The RMS sum of the two σ's is 8.0 dB.

D. Influence of Wind Conditions

In the long-duration path-loss measurements of Experiments 3 and 4, we simultaneously measured wind speed at the base and terminal locations. The wind speed data were recorded every second and later averaged, in offline processing, over 15-min intervals. Here, we present some illustrative results based on 24-h records for each of the six New Jersey locations (a data subset of Experiment 3) and a single 48-h record

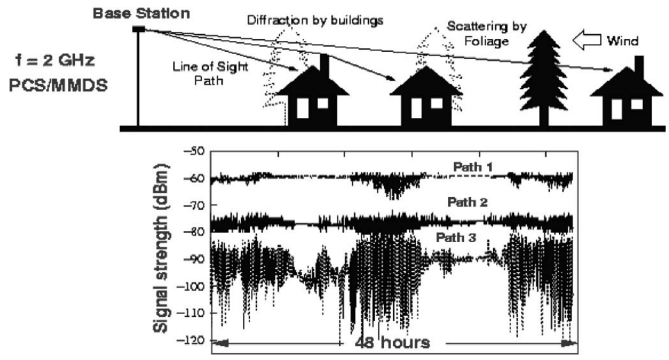

Fig. 12. Simultaneous fading observed on three fixed links in Naperville over a 48-h period.

during which fading on links to three Naperville locations were simultaneously observed (a data subset of Experiment 4).

The observation by us and others, e.g., [6]–[9], that higher wind speeds lead to lower K-factors is consistent with the picture of leaves, branches, and other objects moving in the wind and causing time variations in the sum of received rays. In our results, the correlation between wind speed at the base and the decibel K-factor was found to be -0.47; that between wind speed at the terminal and the decibel K-factor was found to be -0.56. These negative correlations are in line with our intuitive expectations.

Fig. 10 shows a scatter plot of K and wind speed, where the inverse correlation is in evidence. Each point is for a 15-min segment, and there were 96 such segments at 60 frequencies for each of the six terminal locations. For this data set, Fig. 11 shows the manner in which the mean of the K-factor (in decibels) decays with wind speed, calculated in the following wind speed intervals (in kilometers per hour): 0 (no discernible wind), (0, 2], (2, 4], (4, 8], and (8, 16]. The midpoint values of these intervals were chosen as the wind speed points on the abscissa. The steady decrease in the number of data points that we see at higher wind speeds makes it difficult to reliably estimate the standard deviation of K as a function of wind speed. Instead, we simply note that the standard deviations observed for no discernible wind is approximately 5.5 dB and that the global value over all other speeds is approximately 5.2 dB. The seemingly larger spread at zero wind speed (Fig. 10) is a result of the very large number of data points, i.e., as the number of points increases, and so does the likelihood of seeing the more extreme low-probability values.

Fig. 12 shows the signal fading experienced over a 48-h period on three different non-line-of-sight paths, from a 25-m-high base station in Naperville, IL, to three residences located within a 45° sector at distances of 600, 1000, and 1200 m. The first two paths are each obstructed by trees and structures located a few hundred meters away from the remote terminal; the latter path is obstructed by a large stand of trees that is located a few tens of meters from the remote terminal. The simultaneous onset of distinct fading events on the three links is clearly visible, but the depth of fading increases as the path becomes increasingly harsh. The high correlation between fading events on different links within the same cell has implications for radio resource management in fixed wireless systems.

We do not offer the partial results given here as a model for the dependence of K upon wind speed. We merely use them to illustrate an important physical relationship. For a meaningful model development, considerably more experimental data would be required.

V. Conclusion

We have theorized and demonstrated that narrow-band channels in fixed wireless systems can be well modeled by Ricean fading, and we have shown a simple accurate way to compute Ricean K-factors from time records of path gain magnitude. The K-factor is a key indicator of the severity of fading; therefore, modeling its statistics over fixed wireless environments is essential to the study of systems using either narrow-band or multicarrier radio techniques.

To this end, we have described the collection and reduction of a large body of data at 1.9 GHz for suburban paths in New Jersey, Illinois, and Washington. Whereas other studies have focused on locations and scenarios in which moving vehicles and pedestrians have a significant effect on fixed wireless links, we have focused on quiet residential areas where windblown trees and foliage appear to have the most significant impact. We have developed a statistical model that presents K as lognormal over time, frequency, and user location in such environments, with the median being a simple function of season, antenna height, antenna beamwidth, and distance. Moreover, we have separated the variability about the median into two parts: one due to time and frequency variations per location and one due to changes among locations. We have also demonstrated the consistency of key results across different experiments. Finally, we have produced results on the relationship of the K-factor to wind conditions. The results will be useful to those engaged in the design of fixed wireless systems and/or the modeling of fixed wireless channels.

Acknowledgment

We are indebted to numerous past and present AT&T colleagues and contractors for collecting and processing the large quantities of path loss data used in this study. They are D. J. Barnickel, M. K. Dennison, B. J. Guarino, P. B. Guerlain, D. Jacobs, S. C. Kim, R. S. Roman, A. J. Rustako, Jr., S. K. Wang, J. Lee, L. Roberts and M. Stephano.

References

[1] D. Greenwood and L. Hanzo, "Characterization of mobile radio channels," in *Mobile Radio Communications*, R. Steele, Ed. London, U.K.: Pentech, 1992, pp. 163–185.

[2] M. Schwartz, W. R. Bennett, and S. Stein, *Communication Systems and Techniques*. New York: McGraw-Hill, 1966, sec. 9.2.

[3] J. D. Parsons, *The Mobile Radio Propagation Channel*. Hoboken, NJ: Wiley, 1992, pp. 134–136.

[4] W. C. Jakes, Jr., Ed., *Microwave Mobile Communications*. New York: Wiley, 1974.

[5] M. J. Gans, N. Amitay, Y. S. Yeh, T. C. Damen, R. A. Valenzuela, C. Cheon, and J. Lee, "Propagation measurements for fixed wireless loops (FWL) in a suburban region with foliage and terrain blockages," *IEEE Trans. Wireless Commun.*, vol. 1, no. 2, pp. 302–310, Apr. 2002.

[6] E. R. Pelet, J. E. Salt, and G. Wells, "Effect of wind on foliage obstructed line-of-sight channel at 2.5 GHz," *IEEE Trans. Broadcast.*, vol. 50, no. 3, pp. 224–232, Sep. 2004.

[7] D. Crosby, V. S. Abhayawardhana, I. J. Wassell, M. G. Brown, and M. P. Sellars, "Time variability of the foliated fixed wireless access channel at 3.5 GHz," in *Proc. IEEE VTC*, May 30–Jun. 1, 2005, pp. 106–110.

[8] M. H. Hashim and S. Stavrou, "Measurements and modeling of wind influence on radiowave propagation through vegetation," *IEEE Trans. Wireless Commun.*, vol. 5, no. 5, pp. 1055–1064, May 2006.

[9] H. Suzuki, C. D. Wilson, and K. Ziri-Castro, "Time variation characteristics of wireless broadband channel in urban area," in *Proc. 1st Eur. Conf. Antennas Propag.*, Nice, France, Nov. 2006.

[10] L. Ahumada, R. Feick, and R. A. Valenzuela, "Characterization of temporal fading in urban fixed wireless links," *IEEE Commun. Lett.*, vol. 10, no. 4, pp. 242–244, Apr. 2006.

[11] R. P. Torres, B. Cobo, D. Mavares, F. Medina, S. Loredo, and M. Engels, "Measurement and statistical analysis of the temporal variations of a fixed wireless link at 3.5 GHz," *Wireless Pers. Commun.*, vol. 37, no. 1/2, pp. 41–59, Apr. 2006.

[12] R. Feick, R. A. Valenzuela, and L. Ahumada, "Experiment results on the level crossing rate and average fade duration for urban fixed wireless channels," *IEEE Trans. Commun.*, vol. 9, no. 1, pp. 175–179, Jan. 2007.

[13] L. J. Greenstein, S. S. Ghassemzadeh, V. Erceg, and D. G. Michelson, "Ricean K-factors in narrowband fixed wireless channels," in *Proc. WPMC*, Amsterdam, The Netherlands, 1999.

[14] V. Erceg, "Channel models for fixed wireless applications," *IEEE 802.16 Broadband Wireless Access Working Group, IEEE 802.16a-03/01*, Jun. 27, 2003.

[15] L. J. Greenstein, D. G. Michelson, and V. Erceg, "Moment-method estimation of the Ricean K-factor," *IEEE Commun. Lett.*, vol. 3, no. 6, pp. 175–176, Jun. 1999.

[16] C. Tepedelenlioglu, A. Abdi, and G. B. Giannakis, "The Ricean K factor: Estimation and performance analysis," *IEEE Trans. Wireless Commun.*, vol. 2, no. 4, pp. 799–810, Jul. 2003.

[17] Y. Chen and N. C. Beaulieu, "Maximum likelihood estimation of the K factor in Ricean fading channels," *IEEE Commun. Lett.*, vol. 9, no. 12, pp. 1040–1042, Dec. 2005.

[18] V. Erceg, L. J. Greenstein, S. Y. Tjandra, S. R. Parkoff, A. Gupta, B. Kulic, A. A. Julius, and R. Bianchi, "An empirically based path loss model for wireless channels in suburban environments," *IEEE J. Sel. Areas Commun.*, vol. 17, no. 7, pp. 1205–1211, Jul. 1999.

[19] V. Erceg, D. G. Michelson, S. S. Ghassemzadeh, L. J. Greenstein, A. J. Rustako, Jr., P. B. Guerlain, M. K. Dennison, R. S. Roman, D. J. Barnickel, S. C. Wang, and R. R. Miller, "A model for the multipath delay profile of fixed wireless channels," *IEEE J. Sel. Areas Commun.*, vol. 17, no. 3, pp. 399–410, Mar. 1999.

[20] S. R. Hanna and J. C. Chang, "Representativeness of wind measurements on a mesoscale grid with station separations of 312 m to 10 km," *Boundary-Layer Meteorol.*, vol. 60, no. 4, pp. 309–324, Sep. 1992.

[21] M. F. Ibrahim and J. D. Parsons, "Signal strength prediction in built-up areas. Part l: Median signal strength," *Proc. Inst. Elect. Eng.—F*, vol. 130, no. 5, pp. 377–384, Aug. 1983.

Larry J. Greenstein (S'59–M'67–SM'80–F'87–LF'02) received the B.S., M.S., and Ph.D. degrees in electrical engineering from the Illinois Institute of Technology, Chicago, in 1958, 1961, and 1967, respectively.

From 1958 to 1970, he was with IIT Research Institute, Chicago, working on radio frequency interference and anticlutter airborne radar. He joined Bell Laboratories, Holmdel, NJ, in 1970. He was with AT&T for 32 years, conducting research on digital satellites, point-to-point digital radio, optical transmission techniques, and wireless communications. For 21 years during that period (1979–2000), he led a research department renowned for its contributions in these fields. He is currently a Research Scientist with the Wireless Information Network Laboratory (WINLAB), Rutgers University, North Brunswick, NJ, working in the areas of ultrawideband, sensor networks, multiple-input–multiple-output-based systems, broadband power line systems, and radio channel modeling. He has been a Guest Editor, Senior Editor, and Editorial Board Member for numerous publications.

Dr. Greenstein is an AT&T Fellow. He is a recipient of the IEEE Communications Society's Edwin Howard Armstrong Award and a corecipient of four best paper awards. He is currently the Director of Journals for the IEEE Communications Society.

Saeed S. Ghassemzadeh (S'88–M'91–SM'02) received the B.S., M.S., and Ph.D. degrees in electrical engineering from the City University of New York, New York, in 1989, 1991, and 1994, respectively.

From 1989 to 1992, he was with SCS Mobilecom, which is a wireless technology development company, where he conducted research in the areas of wireless channel modeling. In 1992, while working toward the Ph.D. degree, he joined InterDigital, where he worked as a Principal Research Engineer, conducting research in the areas of fixed/mobile wireless channels, and was involved in system integration and testing of B-code-division multiple access (CDMA) technology. At the same time, he was also an Adjunct Lecturer with the City University of New York. In 1995, he joined AT&T Wireless Communication Center of Excellence, AT&T Bell Laboratories, where he was involved in the design and development of the fixed wireless base station. He also conducted research in areas of CDMA technologies, propagation channel measurement and modeling, satellite communications, wireless local area networks, and coding in wireless systems. He is currently Principal Member of Technical Staff with the Communication Technology Research Department at AT&T Labs-Research, Florham Park, NJ. His current research interest includes wireless propagation measurement and modeling, cognitive radio, wireless local area networks, and terahertz communications.

Dr. Ghassemzadeh is a member of the IEEE Communication Society and IEEE Vehicular Technology Society. He is currently an Associate Editor for the IEEE TRANSACTIONS ON WIRELESS COMMUNICATIONS and the *Journal of Communications and Networks*.

Vinko Erceg (M'92–SM'98–F'07) received the B.Sc. degree in electrical engineering and the Ph.D. degree in electrical engineering from the City University of New York, in 1988 and 1992, respectively.

From 1990 to 1992, he was a Lecturer with the Department of Electrical Engineering, City College of the City University of New York. Concurrently, he was a Research Scientist with SCS Mobilecom, Port Washington, NY, working on spread-spectrum systems for mobile communications. In 1992, he joined AT&T Bell Laboratories. In 1996, he joined AT&T Labs—Research as a Principal Member of Technical Staff with the Wireless Communications Research Department, where he worked on signal propagation and other projects related to the systems engineering and performance analysis of personal and mobile communication systems. From 2000 to 2002, he was with Iospan Wireless Inc., San Jose, CA, as the Director of the Communication Systems Division, working on system, propagation, deployment, and performance issues of a multiple-input–multiple-output orthogonal frequency division multiplexing communication system. He is currently a Senior Manager with the Broadcom Corporation, San Diego, CA.

David G. Michelson (S'80–M'89–SM'99) received the B.A.Sc., M.A.Sc., and Ph.D. degrees in electrical engineering from the University of British Columbia (UBC), Vancouver, BC, Canada.

From 1996 to 2001, he served as a member of a joint team from AT&T Wireless Services, Redmond, WA, and AT&T Labs—Research, Red Bank, NJ, where he was concerned with the development of propagation and channel models for next-generation and fixed wireless systems. The results of this work formed the basis for the propagation and channel models later adopted by the IEEE 802.16 Working Group on Broadband Fixed Wireless Access Standards. From 2001 to 2002, he helped to oversee the deployment of one of the world's largest campus wireless local area networks at UBC while also serving as an Adjunct Professor with the Department of Electrical and Computer Engineering. Since 2003, he has led the Radio Science Laboratory, Department of Electrical and Computer Engineering, UBC, where his current research interests include propagation and channel modeling for fixed wireless, ultra wideband, and satellite communications.

Prof. Michelson is a registered professional engineer. He serves as the Chair of the IEEE Vehicular Technology Society Technical Committee on Propagation and Channel Modeling and as an Associate Editor for Mobile Channels for *IEEE Vehicular Technology Magazine*. In 2002, he served as a Guest Editor for a pair of Special Issues of the IEEE JOURNAL ON SELECTED AREAS IN COMMUNICATIONS concerning propagation and channel modeling. From 2001 to 2007, he served as an Associate Editor for the IEEE TRANSACTIONS ON VEHICULAR TECHNOLOGY. From 1999 to 2007, he was the Chair of the IEEE Vancouver Section's Joint Communications Chapter. Under his leadership, the chapter received Outstanding Achievement Awards from the IEEE Communications Society in 2002 and 2005 and the Chapter of the Year Award from IEEE Vehicular Technology Society in 2006. He received the E. F. Glass Award from IEEE Canada in 2009.